Noncontact Determination of Fluid Properties by Means of Focused Acoustics

Senior Honors Thesis

Zach Capalbo, Department of Physics, Gordon College, Wenham, MA

05/15/2012

"One cannot reflect in streaming water. Only those who know internal peace can give it to others."

— Lao Tzu

Abstract

A focused acoustic transducer is used to form a small mound on the surface of a water glycol solution. The transducer is then used to ultrasonically measure the height of the mound at successive intervals as the mound relaxes. The relaxation curve can be used to determine the surface tension of the solution. Various concentrations of water and glycol are analyzed, and the results compared with surface tensions for known concentrations.

Contents

List of Figures

Part I
Overview

The use of focused acoustic waves provides a powerful tool for investigations in fluid dynamics. Both manipulation and measurement is possible with focused acoustics. The ability to manipulate and measure the fluid with the same apparatus unlocks useful potential to integrate the two into a convenient single apparatus.

The possibility for acoustic waves to transmit through fluid containers provides a compelling reason to investigate the use of focused acoustics in fluids research. Viscosity and surface tension provide two of the main forces acting on fluids, as well as being important and useful properties of a fluid. Thus, a non-contact method for measurement of these properties provides both a promising and useful application of focused acoustics.

This topic centers on the intersection of fluid dynamics and nonlinear acoustics, and reaches into the boundaries of thermodynamics and chemistry. It is a topic that has been explored in the literature, yet many gaps in our knowledge still remain—to say nothing of the new frontiers emerging.

1 History and Other Methods

Viscosity and surface tension have been widely studied phenomena throughout history, and several methods developed for their measurements.

1.1 Viscometry

A common method for measuring viscosity is through the use of capillary tubes. In the capillary viscometry method, the time is measured for a known volume of fluid to flow through a capillary of known diameter and length. One can also measure the pressure of a constantly flowing liquid through the cylinder at different cylindrical radii to determine viscosity (Wilke et al., 2000).

Another method for determining viscosity is the falling ball method. In this method, a ball is dropped in a small cylinder of a fluid. The shear viscosity can then be determined by measuring the terminal viscosity of the ball as it falls. In the limiting case of an infinite fluid, the terminal velocity (v_t) and viscous drag force (F_D) are linearly related by the equation

$$F_D = 6\pi r \mu_\infty v_t$$

where r is the radius of the ball, and μ_∞ is the coefficient of dynamic viscosity. The walls of a finite diameter cylinder will yield much more complicated results (Vikram Singh et al., 2012). More novel approaches include using optical tweezers to measure viscosity of picolitre volume fluids (Parkin et al., 2007).

Ultrasonic techniques are also widely used to determine viscosity. For instance, viscosity can be measured by measuring the Doppler shift of an ultrasonic pulse sent

through a flowing fluid (Koseli et al., 2006), or by immersing a transducer and measuring changes in radiation load resistance, resonant frequency, and phase shift between pressure and flow velocity (Heuter and Bolt, 2000).

1.2 Surface Tension Measurements

One venerable method for measuring surface tension is to immerse a very thin ring in the liquid, and then measure the force needed to pull the ring out of the fluid (du Noüy, 1925). Another method involves immersing a plate in the liquid and measuring the force on the plate. The surface tension can then be calculated using the equation

$$\gamma = \frac{F}{l \cdot \cos\theta}$$

where γ is the coefficient of surface tension, F is the force due to surface tension, l is the perimeter of the submersed section of the plate, and θ is the contact angle between the plate and the surface of the liquid (Rame, 1996).

Another method to measure surface tension involves the contact angle of a droplet on a wetted surface (Huh and Reed, 1983). By obtaining a clear image of a liquid drop wetting a surface, the angle that the droplet profile makes with the wetted surface can be obtained. From this contact angle and some knowledge of the surface properties, the surface tension can be obtained.

Ultrasonics again find applications in surface tension measurements. A method particularly similar to the present experiment involves using a focused acoustic pulse to form a mound on the surface of the liquid. As the mound collapses, it spreads and forms surface waves. These waves are measured at different points by a laser pointed at the surface. The surface tension can then be determined to high accuracy from the measurement of the frequency of the surface waves (Cinbis and Khuri-Yakub, 1992).

2 Experiment and Theory Run-through

The basic premise of the experiment is that a mound of fluid will decay at a rate that is dependent on the viscosity and surface tension of the fluid. By using focused acoustic waves below the surface of the fluid using an acoustic transducer, we can cause a mound to form. Using that same transducer, we can use ultrasonic distance measurement techniques to take measurements of the height of the mound as it decays. The rate at which the mound relaxes back to a flat surface will be determined by the surface tension and viscosity of the fluids, and so by looking at the rate at which the mound relaxes, we can determine the surface tension and viscosity of the fluid.

3 Applications

This research would be useful in many different areas of physics, biology, and chemistry. This technique would not involve contacting the liquid with a plate, a ball, or any other object, as is done in most cases. Furthermore, this method would not require

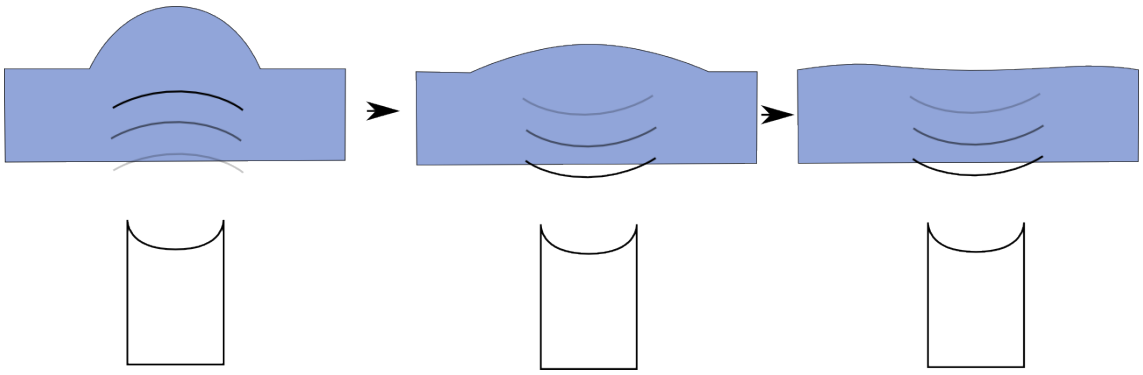

Figure 1: Acoustic pulse used to form mound and measure relaxation

the use of any additional apparatus such as a laser, but would require only a single transducer. Also, since the diameters of the mounds are on the order of millimeters, only a very small amount of fluid actually need be used. Finally, if the liquid container is a close acoustic match to water, the fluid does not even need to leave the container. This is a huge advantage over most other methods which require liquid to flow through special apparatuses or sit in special compartments.

The method could easily be worked into chemistry or biological assay arrays, where very large numbers of very small amounts of fluids are tested for different properties. Much already existing equipment has been designed to pass well plates—which can contain hundreds or thousands of fluids to test—at high speeds over acoustic transducers (Dryer et al., 2011). It should be fairly straight forward to modify these apparatus or even merely change the control software to include mound formation and relaxation tests for surface tension and viscosity.

Part II
Theory

4 Acoustics

4.1 Electric Power

The power delivered by a sinusoidal wave pulse is $\frac{V_{rms}^2}{R}$, and the V_{rms} for a sinusoidal wave is $\frac{V_0}{\sqrt{2}}$ (Nilsson and Riedel, 2011). Thus the energy delivered by a pulse of duration t is $t\frac{V_0^2}{2R}$. If the pulse is repeatedly delivered at intervals with period $T > t$, then the average power delivered by the wave is given by

$$\frac{t}{T}\frac{V_0^2}{2R}$$

4.2 Attenuation

As acoustic waves travel in a dissipative medium, the acoustic pulse attenuates, or looses intensity. This is often due to viscous intermolecular forces dissipating the acoustic energy. The intensity of an acoustic wave decays exponentially along the axis of travel according to the form

$$I_d = I_0 e^{-2\alpha d}$$

where d is the distance along the axis of travel, I_d is the intensity at d, I_0 is the initial intensity, and α is a constant decay factor which depends on the properties of the material (Nowicki et al., 1997).

4.3 Reflection and transmission

When an acoustic wave encounters and interface between two media, some of the amplitude is reflected and some is transmitted. The intensity of reflection or transmission depends on the difference in acoustic impedance between the two materials. Intensity of the transmitted wave is given by

$$\frac{I_t}{I_i} = \left(\frac{Z_1 - Z_2}{Z_1 + Z_2}\right)^2$$

where I_t is the transmitted intensity, I_i is the incident intensity, Z_1 is the impedance of the source medium, and Z_2 is the acoustic impedance of the transmission medium (NDT International, Inc., 2010).

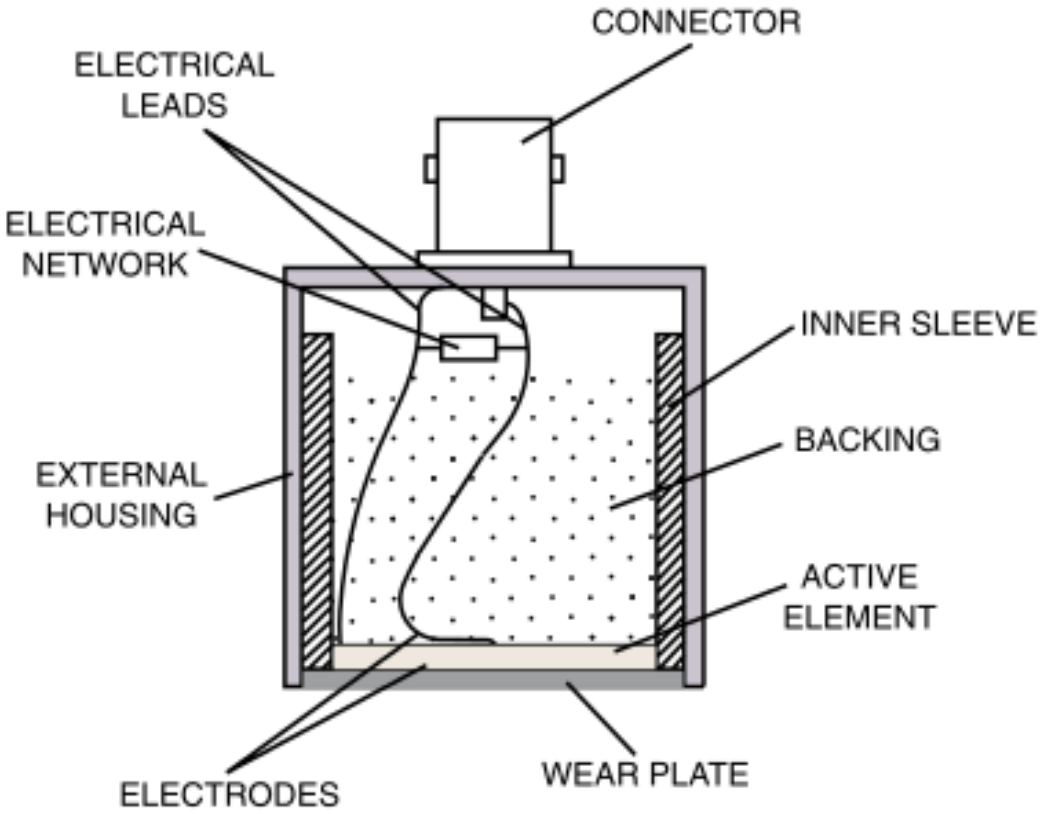

Figure 2: Piezoelectric transducer diagram (NDT International, Inc., 2010)

5 Piezoelectric Transducers

A piezoelectric material is a material which expands or contracts when a voltage is applied across it, and likewise produces an electric voltage when it experiences a normal stress. This property can be used to generate acoustic waves. An acoustic transducer is made of a piezoelectric active element and other elements to direct the acoustic waves in a controlled manner. The active element is attached to a wear plate which faces outward in the direction that the acoustic waves will travel. In the opposite direction, the active element is attached to a damping material. This serves two purposes. One is to direct the waves outward through the wear plate, and the other is to dampen the vibrations of the active element so that it does not vibrate spuriously.

However, because the damping must be low enough to allow the acoustic waves

to vibrate the piezo element, the vibrations will be under-damped oscillations. These extra, decaying oscillations are known as ringdown, and are clearly seen in Figure 12 and Figure 13.

5.1 Resolution Vs. Sensitivity

Ultrasonic transducers are generally produced as either high resolution or high sensitivity. The differences between high resolution and high sensitivity transducers are due to the different damping applied to each. The damping affects a number of different transducer characteristics, most notably ringdown—the amount of extra vibrations of the transducer surface when receiving an acoustic signal—and bandwidth—the sensitivity of a transducer to the frequency of the driving signal.

High resolution transducers are highly damped and broad band. This has the effect of reducing the ring-down associated with an acoustic signal. This provides greater temporal resolution, since the duration of the ring-down is reduced. However, because of the high damping, the acoustic power transferred by a high resolution transducer is considerably less than a corresponding high sensitivity transducer (NDT International, Inc., 2010).

High sensitivity transducers are lightly damped and narrow band. This allows for greater acoustic power transfer, but less temporal resolution. Since the transducer is lightly damped, the duration of the ring-down is much longer. This makes it more difficult to identify a single time of flight. However, since the ring down interacts acoustically with the fluid, it may be possible to gain additional information by analyzing the shape of the ringdown (see subsection 23.2).

5.2 Frequency

The frequency of the transducer is determined by the length of the piezoelectric active element. The active element is cut to half of the wavelength of the transducer. This frequency is then the resonant frequency of the transducer. The transducer resonance will also have a bandwidth, which depends largely on the damping material used in the transducer. High resolution transducers will have a large bandwidth, while high sensitivity transducers will have a narrow bandwidth.

5.3 Power Transfer

The power conversion efficiency transducer is defined as

$$\eta = \frac{\text{power radiated into load}}{\text{total input power}}$$

(Heuter and Bolt, 2000). η depends largely on the material of the wear plate. For quartz, which is a common material choice, $\eta \approx 62\%$.

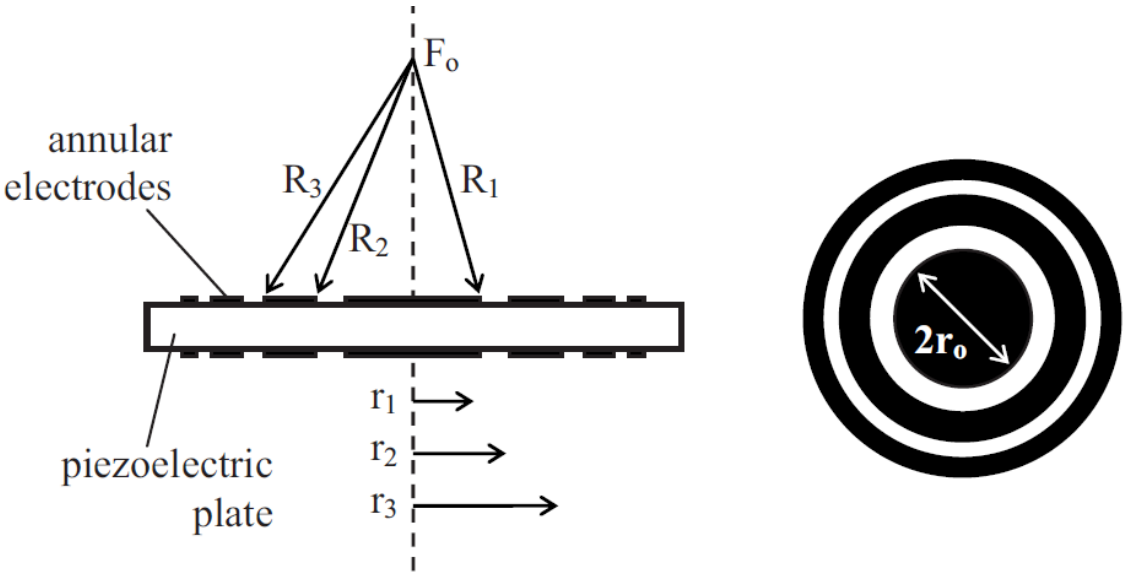

Figure 3: Diagram of side and top view of a Fresnel Zone Plate (Hon, 2009)

5.4 Acoustic Phased Arrays

One method of focusing acoustic waves is the acoustic phased array. This method relies on constructive and destructive interference of acoustic waves to produce a focus. In an acoustic phased array, several transducers are gathered side by side. When an acoustic pulse is to be sent, a slight time delay, causing a phase shift, is inserted in the signal sent to some of the transducers. This phase shift will cause interference patterns in the emitted waves. If the phase shift is carefully controlled, the acoustic waves can be caused to all constructively interfere at a small location with a radius of the wavelength of the signal (NASA, 1998).

Acoustic phased arrays offer the flexibility of being able to change the focus, and even direct the focus in different directions, all depending on the way the phase shift is inserted into the signals (NASA, 1998).

5.5 Fresnel Zone Plates

Fresnel Zone Plates reduce the idea of constructive interference to a single transducer. The Fresnel Zone Plate is milled as a sort of lense on the transducer, which works essentially like a diffraction grating. The plate is a flat milled piece that causes interference in such a way that the wave constructively interferes with itself at the focal point (Hon, 2009).

5.6 Spherically Focused Transducer

In a spherically focused transducer, the quartz buffer rod is shaped by grinding and polishing at the end to form a part of a sphere, focusing the acoustic waves much like a satellite or a lens does for electromagnetic waves. The focusing effect will cause the acoustic waves to have maximum amplitude exactly at the focal spot, which is the point one focal length along the transducer axis. The maximum intensity will be in this small area, which is roughly the diameter of the wavelength of the of the acoustic wave in the liquid. Around the focal point orthogonal to the transducer axis, there will be a very low intensity. Elsewhere, the acoustic waves will be dispersed, leading to lower intensity, but spread out over a wider area.

5.7 Acoustic Impedance

An immersion transducer is produced so that the acoustic impedance of the transducer is a close match to the acoustic impedance of water. This allows the transducer to have good power transfer even when it is immersed underwater or in a liquid with an acoustic impedance close to that of water. However, if the transducer is exposed to air, then there will be a strong impedance mismatch, and nearly all of the energy will be reflected back into the active element, possibly damaging the transducer.

6 Fluid Dynamics

The fundamental equation in fluid dynamics—analogous to Newton's second law in classical mechanics—is the Navier-Stokes equation, which commonly takes the form

$$\rho \frac{Dv}{Dt} = -\nabla p + \nabla \cdot \mathbf{T} + f$$

where ρ is the density of the fluid, $\frac{Dv}{Dt}$ is the material derivative of the velocity, p is the pressure, and T is the stress tensor. This equation can be derived from the conservation of mass principles (Enflo and Hedberg, 2002). Fortunately, a complete solution is not necessary to understand the experiment.

6.1 Viscosity

Viscosity is the tangential stress per unit meter of a fluid (Heuter and Bolt, 2000). It can be thought of as the resistance of the particles of a fluid to flowing past one another. There are two types of viscosity, shear and volume. Shear viscosity relates to fluid particles flowing past one another, as when two parallel plates with fluid between them are slid in opposite directions. Volume viscosity relates to compression of the fluid, but for most purposes, its effect is negligible compared to shear viscosity.

Viscosity is the main cause of absorption of acoustic waves in liquids (Heuter and Bolt, 2000). Acoustic attenuation in a medium along the axis of travel is given by

$$I_z = I_0 e^{-\alpha z}$$

where z is the distance along the axis of travel, I_0 is the incident intensity, and for a viscous medium, α is given by

$$\alpha \approx \frac{2}{3}\frac{\eta}{\rho}\frac{\omega^2}{c^2}$$

where η is the shear viscosity of the medium, ω is the frequency of the wave, and c is the sound speed in the medium.

6.2 Surface Tension

Surface tension can be defined in a few different ways. One way is

$$\sigma = \frac{\text{Work to increase surface area}}{\text{Increase in surface area}}$$

(Heuter and Bolt, 2000). And so, immediately we can see that in order to create a mound with surface area A, the energy that need be applied to overcome the force of surface tension is σA.

It can also be defined as

$$\sigma = \frac{\text{Force}}{\text{Unit Length}}$$

showing that surface tension exerts a force on the surface as it is deformed a length away from the minimum surface area position.

Taken together, these two definitions can explain most of the experiment. A certain amount of energy is needed to be put into the surface in order to create a mound of surface area A. Then, as this energy is switched off, surface tension operates as a restoring force, pushing the surface back to its flat, original configuration (Elrod et al., 1989).

7 Propylene Glycol

Propylene Glycol is a common ingredient in many applications such as plastics, industrial coolants, paints, inks, pharmaceuticals, and foods (Dow Chemical Company, 2003). The main chemical properties of propylene glycol come from the two hydroxyl groups (See Figure 4). This gives propylene glycol chemical characteristics between an alcohol and glycerin (Dow Chemical Company, 2003). Further, it has very high solubility in water. For the purposes of this experiment, however, the only chemical characteristics that will be relevant are the speed of sound, viscosity (Figure 5) and surface tension (Figure 6).

The speed of sound in pure propylene glycol is 1531 m/s (FLEXIM, 2006). Since a detailed study of the dependence of speed of sound on concentration in an aqueous solution was not available, an assumption of a linear dependence was made. Since this speed of sound is very close to the speed of sound in water (1484 m/s), this approximation should be reasonably accurate.

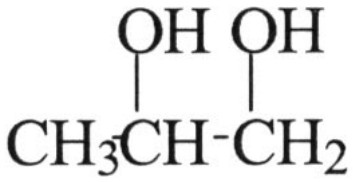

Figure 4: Chemical Structure of Propylene Glycol. (Dow Chemical Company, 2003)

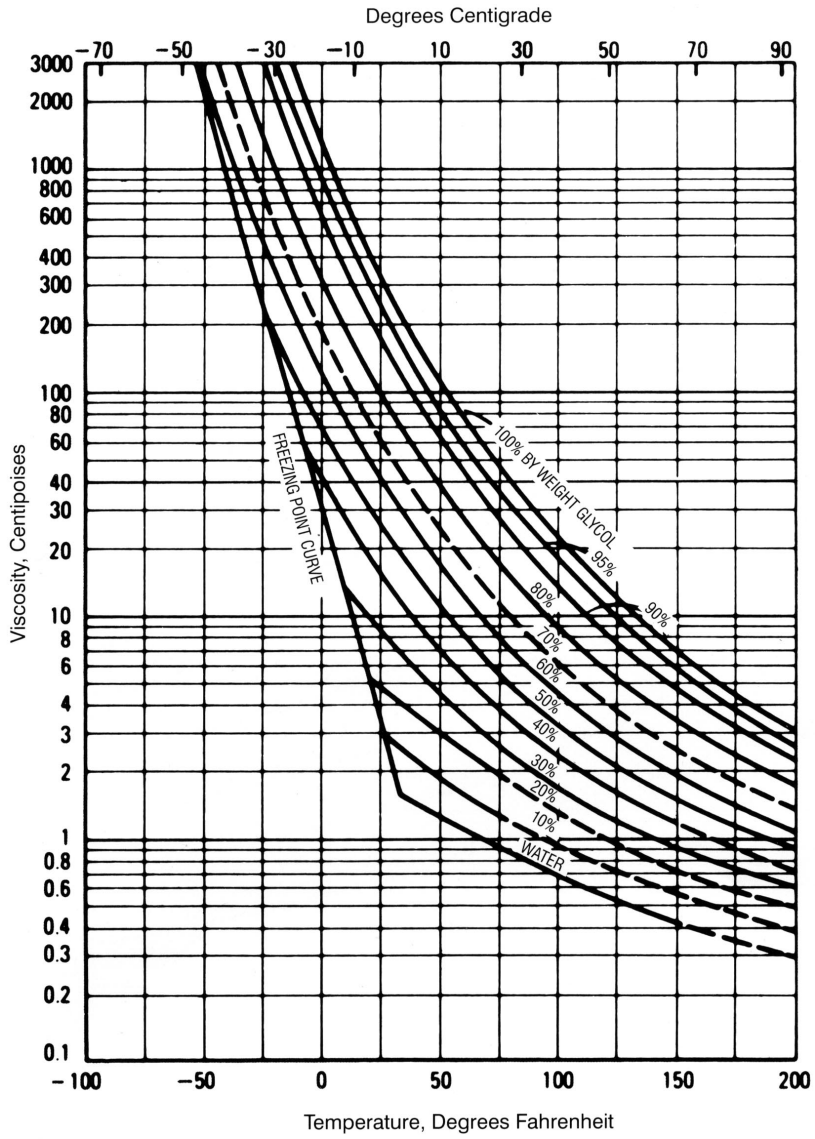

Figure 5: Viscosity of Water and Propylene Glycol solutions. (Dow Chemical Company, 2003)

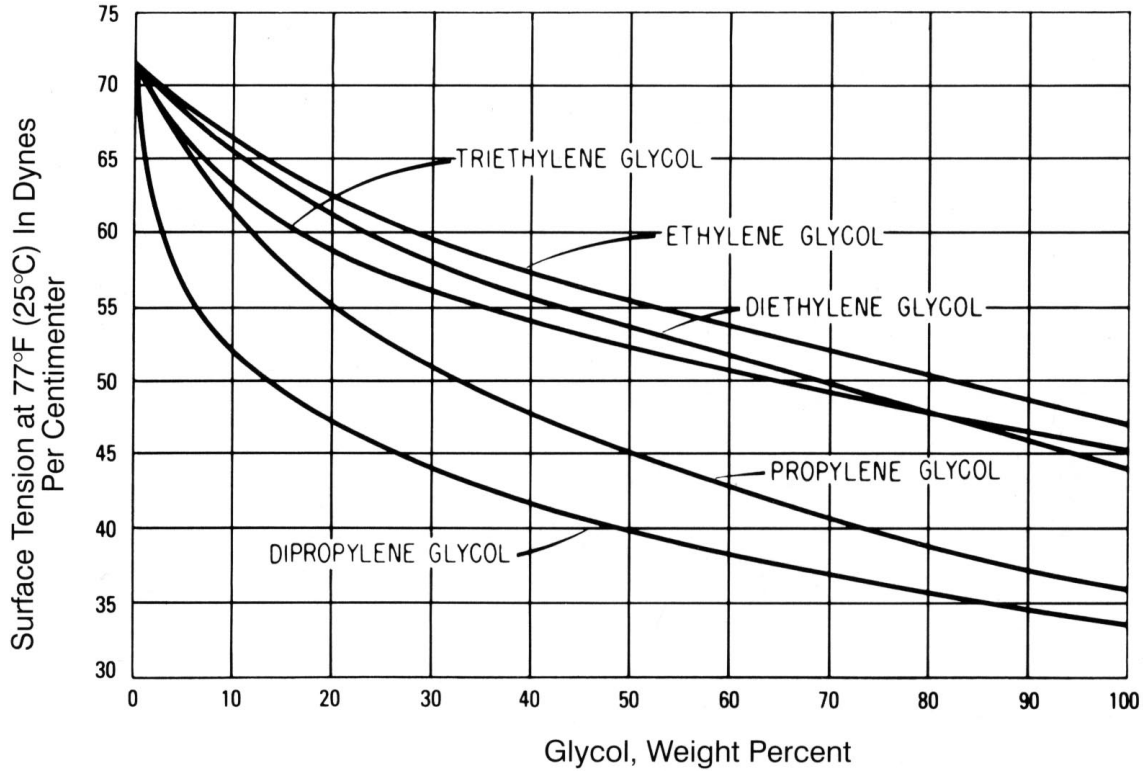

Figure 6: Surface Tension of Water and Propylene Glycol solutions. (Dow Chemical Company, 2003)

8 Ultrasonics

Ultrasonics is the principle of using ultrasound waves to determine properties of a material or object. There is no strict cut off for ultrasonic frequencies, but generally any frequencies above human hearing (20 kHz) up through the Gigahertz range fall under the umbrella of ultrasound. Ultrasonics can be used for measuring viscosity or surface tension (see section 1), creating fog or vapor, or even locating fish in a lake (Inouchi and Shibata, 2008). By far the most common use, however, of ultrasonics is distance measurement.

The basic principle of ultrasonic distance measurement is that ultrasonic acoustic waves will propagate at a known velocity through a medium, then reflect at the interface of that medium and another. The reflected wave will then travel back through that medium at that same velocity. Thus the distance that the ultrasonic wave traveled in that medium can be determined by

$$D = \frac{\Delta t}{2} v_s$$

where Δt is the time between sending and receiving the pulse, and v_s is the speed of sound in that medium (NDT International, Inc., 2010). Since not all of the wave will be reflected at the interface, some of the wave may be transmitted through to the next interface, allowing distance of multiple materials adjacent to one another.

8.1 ADE

Acoustic Droplet Ejection is a common use of focused ultrasound. Instead of simply forming a mound, the energy is enough to actually cause a droplet to fly off of the surface of the liquid. Acoustic droplet ejection has been widely studied and forms the basis for many important ultrasound applications.

9 Mounds

When enough energy is applied to the surface of a liquid to overcome the forces of gravity and surface tension, the surface of the liquid is propelled upward, forming a bump or a mound.

9.1 Formation

As the incident acoustic waves encounter the liquid surface to air interface, it carries a certain pressure with it. The pressure that is felt upon the surface of the liquid is known as Langevin radiation pressure, and is given by

$$P_L = \frac{2I_i}{c}$$

where P_L is the Langevin radiation pressure, I_i is the incident intensity, and c is the speed of sound in the liquid (Cinbis et al., 1993). When the liquid surface is at the

focus of the transducer, this pressure is confined to the small area of the focal spot of the transducer, which then feels and upward force. When this force overcomes the forces of gravity and surface tension, the area will begin to rise, forming a mound with initial momentum

$$p_{init} = P_L AT = \frac{2AI_iT}{c} = \frac{2E}{c}$$

where A is the area of the focal spot (very close to the wavelength of the wave in the fluid), T is the duration of the acoustic pulse, and E is the energy incident in the burst (Elrod et al., 1989).

Mound formation is highly dependent on the position of the fluid surface with respect to the transducer focal point. If the surface is out of focus, the acoustic waves will not be focused, rather they will be more dispersed, which means the energy will be spread over a larger spatial extent, leading to a wider mound with less energy per unit area. The smallest possible mound diameter (which will be roughly the size of the focal spot), will occur exactly at the focus (Hon, 2009).

By analyzing the unstable Bernoulli's equation, Cinbis et al. were able to derive the following equation for the rise time of a mound at the surface of a liquid at the focus of an ultrasonic transducer:

$$t_r = 0.116\frac{2\lambda^{3/2}F^{3/2}\rho^{1/2}}{\sigma^{1/2}}$$

where t_r is the time it takes for the mound to reach maximum height, λ is the wavelength of sound in the fluid, F is the F number of the transducer, ρ is the density of the liquid, and σ is the surface tension.

By solving for σ, we are left with

$$\sigma = 0.0538\frac{\lambda^3F^3\rho}{t_r^2}$$

9.2 Maximum Height

The maximum height that a mound will reach is given by

$$0.21\frac{E^2f^4}{c^6\sigma\rho}$$

where E is the incident acoustic energy, f is the frequency of the acoustic pulse, c is the speed of sound in the liquid, σ is the surface tension of the liquid, and ρ is the density of the liquid (Elrod et al., 1989)

9.3 Decay

Since the acoustic pulse and the associated radiation pressure are transitory, the forces of gravity and surface tension will begin to restore the surface of the mound to the initial resting state. As the mound relaxes it will also generate capillary waves that propagate radially outward (Cinbis and Khuri-Yakub, 1992).

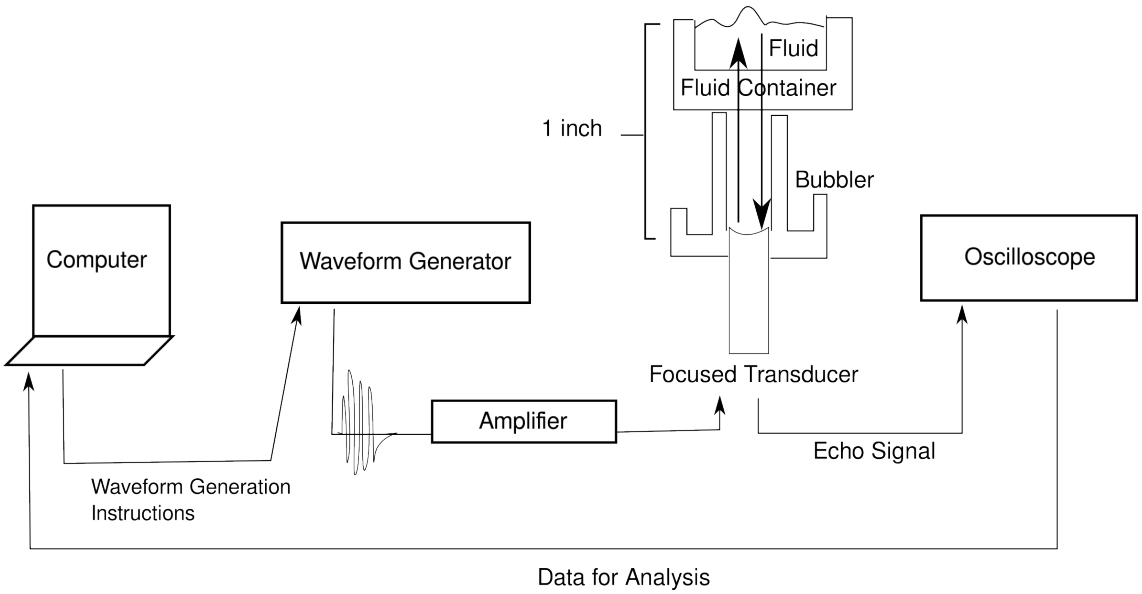

Figure 7: Experimental Setup Diagram

Part III
Experimental Setup

10 Experimental Overview

The experiment is run iteratively. At each iteration, a mound is formed, then there is a delay, and then a single mound height measurement using a single echo pulse is taken. At the next iteration, a new mound is formed, then the duration of the delay is slightly increased, then another single mound height measurement using a single echo pulse is taken. The process repeats for a set number of delays, enough to take enough measurements of the entire rise and fall of the mound.

11 Signal Generation

The first step in the RF train is the signal generation. The pulses are initially created on a computer, downloaded to the waveform generator (Pragmatic 2416A Waveform Generator) via GPIB, then stored in the waveform generator's segment memory.

The actual RF signal is generated by the waveform generator from the pulses stored in memory. It is triggered by an internal timer operating at 1 to 3 Hz. The rate of the timer must be slow enough as not to overstep the safe limits of the transducer power limits.

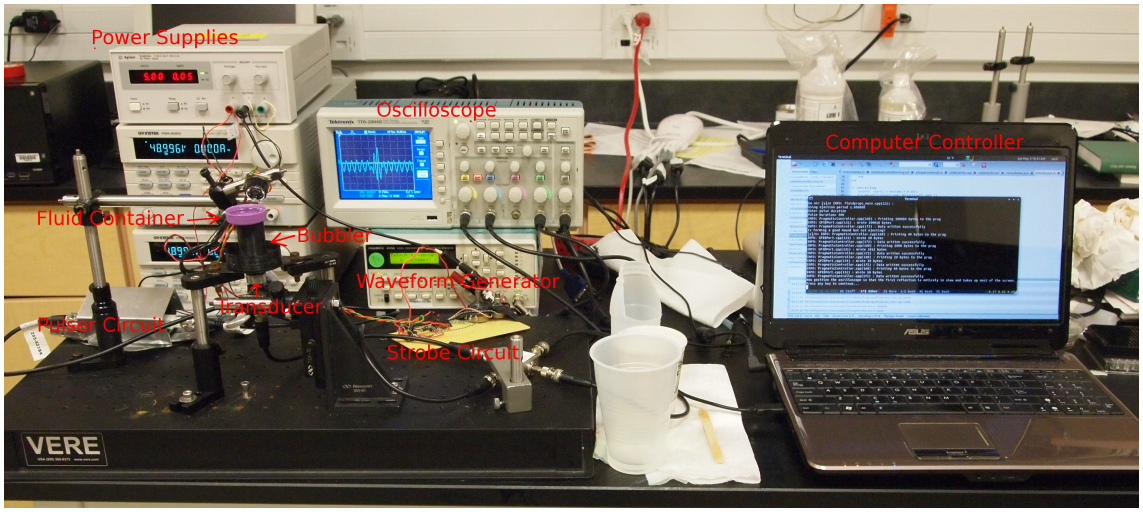

Figure 8: Experimental Setup Photograph

The full pulse consists of three parts, the mound forming pulse, the variable delay, and the echo pulse. These three parts are stored as separate segments, and then combined using the 2416A's sequence functionality.

11.1 Mound Forming Pulse

The pulse emitted to form the mound is a sine wave whose frequency is at or near the resonant frequency of the transducer. The sine wave will have a pulse duration on the order of tens to hundreds of microseconds. The actual duration necessary is dependent on the damping of the transducer and the acoustic impedance between the coupling fluid, fluid container, and test fluid. The pulse may be chirped. That is, it may sweep across frequencies (typically a total range of 1 MHz) centered at the resonant frequency of the transducer. Chirping is designed to reduce standing vibrations.

If too much power is delivered, surface tension will pinch off the top of the mound, and a droplet will be ejected. If this occurs, the power must be lowered, either by using a lower voltage pulse, or a shorter pulse duration. In practice, it is often easiest to find an operative pulse voltage and duration by first ejecting a droplet, and then successively decreasing either the voltage or the pulse duration until a droplet no longer ejects. The most straightforward method for determining whether a droplet or a mound has formed is through visual inspection (see section 17).

11.2 Delay

After the mound pulse is emitted, a delay is inserted. The length of this delay varies from 10 μs to .3 seconds over the course of the experiment. At each iteration, the delay is increased slightly, and then the time of flight for that amount of delay is recorded.

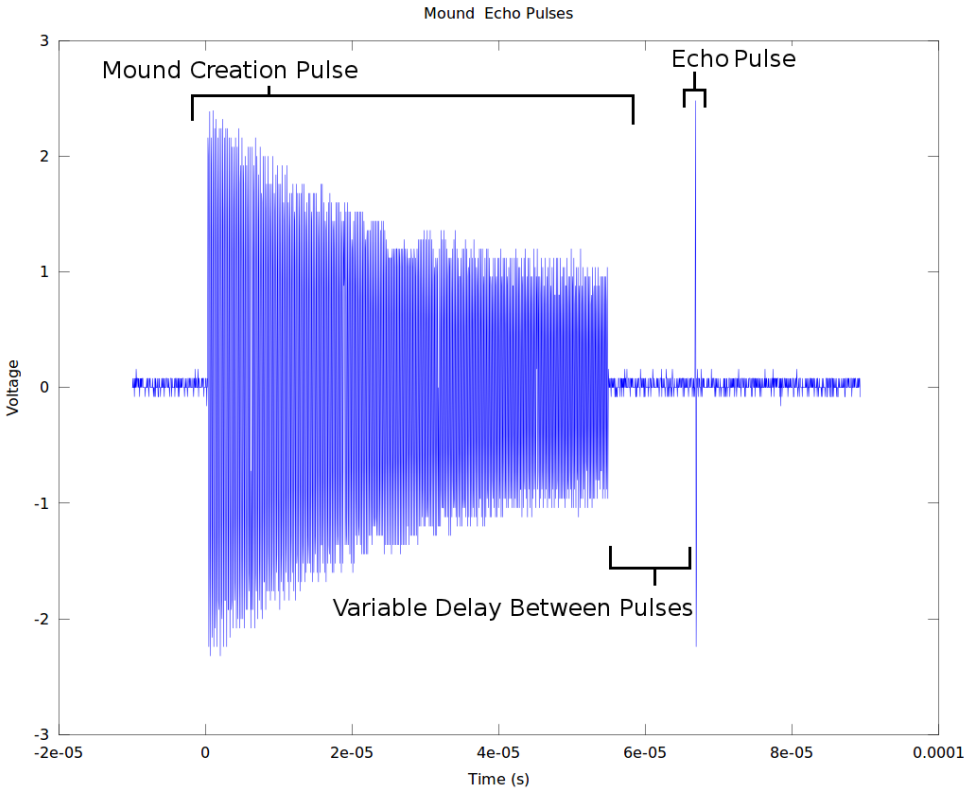

Figure 9: Complete RF Signal to form a mound and send an echo pulse

In this way, the variation in echo delay time provides the time resolution capabilities of this experiment.

The high acoustic power of the mound pulse will cause significant ring down in the transducer. This ring down will persist for several microseconds after the mound pulse has ceased, depending on the damping of the transducer. Combined with the many acoustic reflections generated by the mound pulse, this effect makes reflection of the echo pulse indistinguishable for the the first few microseconds after the ejection pulse. The time needed for the mound to fully settle and equilibrate is on the order of 50 milliseconds.

11.3 Echo Pulse

After the delay, the echo pulse is sent. The echo pulse takes the form of a half-sine wave at the resonant frequency of the transducer. The purpose of this pulse is to provide enough energy to provide a clear reflection at the surface of the fluid, but with a short enough duration to have a clear maximum at a distinct time.

12 Amplification

After the pulse is generated, it must be amplified to have sufficient power to form a mound. The waveform generator produces a 5 Vpp. This is amplified to 98 Vpp using a custom rail-to-rail pulser circuit. The height of the mound formed is proportional to the square of the voltage.

13 Transducer

The transducers used in this setup are focused piezo-electric immersion transducers. They contain a piezo element attached to a quartz buffer rod. The quartz rod is ground at the end into a spherical lens. One transducer was a 5 MHz high resolution transducer, and the other was a 5 MHz high sensitivity transducer.

The focus of the transducer is adjusted by moving the transducer relative to the surface of the fluid. The transducer is mounted on a linear stage. The top part of the transducer forms a sliding seal with the bubbler, which is a cylinder of roughly the length of the transducer focus filled with a coupling fluid. The bubbler is held stationary while the transducer slides up or down in the bubbler. The fluid container is placed on top of the bubbler, and thus the distance between the transducer and the fluid surface can be easily varied.

The transducer is set up so that the surface of the fluid is not directly in focus. Rather, it is either somewhat below, or somewhat above the focus. This will create a mound whose diameter is larger than the wavelength of the echo signal (see subsection 9.1). This will allow the echo signal to be transmitted to and from the top of the mound without any interference.

14 Fluid Coupling

The bubbler is filled with a coupling fluid which transmits the acoustic waves from the transducer to the test fluid. Since some energy will be reflected at both the interface between the transducer and coupling fluid, and coupling fluid and fluid container, the coupling fluid must have an acoustic impedance close to the container of the test fluid as well as to the acoustic impedance of the transducer so as to minimize these reflections. If there is an impedance mismatch, then most of the acoustic energy will be reflected at the coupling fluid interface, leading either to insufficient energy for mound formation, or even to the maximum echo response coming from this interface rather than the fluid surface.

Constant contact must be maintained between the coupling fluid and the test fluid container. Any air bubbles between the transducer and the fluid reservoir will cause a total acoustic reflection at that interface, meaning that no acoustic energy is transferred to the test fluid.

14.1 Water

Because the acoustic impedance of the transducer is matched to water, water is a natural choice to use as the coupling fluid. Further, water has a low viscosity, ensuring that very little acoustic energy is dissipated as the pulse travels the length of the bubbler.

14.2 Fluid Container

Three types of fluid containment were used in these experiments: no container, a plastic petri dish, and an HDPE bottle cap.

Using no container and placing the fluid to be tested directly in the bubbler right on top of the transducer is the most straightforward method for testing the fluid. Since there is no fluid container, there is no power loss due to reflection on the container interface; the maximum power is transferred to the surface of the liquid. Furthermore, there is not the concern about inducing shear waves due to improper alignment of the fluid container on the bubbler. Of course, the drawback is that this method is not entirely a non-contact method, since the liquid is directly on top of and in contact with the transducer. Nonetheless, it is a useful way to verify both the basic tenets of the experiment and the experimental setup.

A plastic lab petri dish was used as a fluid container for some runs of the experiment. They are made out of polypropylene, and have a thin flat bottom. This makes the petri dishes good containers for several reasons. Since the bottoms are flat, they can rest easily on the bubbler. Since they are thin, the acoustic losses in the container, while certainly noticeable, are low enough as to allow enough energy for mound formation to pass through. The plastic has a fairly close impedance match with water, allowing for partial transmission of the acoustic signal. However, the large diameter of the petri dish compared to the bubbler can sometimes make it difficult to align the experiment consistently, since the height of the fluid may vary considerably over the area of the

petri dish if it is not perfectly level. Further, some of the petri dishes have a tendency to bow and flex in the center, leading to possible shear waves due to a non-perpendicular surface.

The other container used was a plastic milk bottle cap, made from High Density Polyethylene. The small size of the bottle caps makes them much easier to handle than the petri dishes. The diameter of the cap is very close to the diameter of the bubbler, so there is little danger of knocking it over and spilling it. Further, the small size of the bottle cap means that on a reasonably level surface, the height of the fluid in the cap should be fairly uniform. Also, the stiffness of the bottle cap prevents bending and flexing, ensuring good acoustic coupling.

15 Fluid

An aqueous solution of propylene glycol is used as the liquid to be tested. Volumes of 5 mL are used in concentrations of 0% to 100% by volume. The solutions are mixed with a wooden mixing stick until it is visibly mixed.

16 Measurement and Control

The time of flight of the acoustic echo pulse in the fluid is measured at each iteration of the experiment. The oscilloscope is triggered to the falling edge of the Waveform generator's trigger pulse. This effectively starts a timer when the echo pulse is sent out. The oscilloscope is then adjusted until the return echo pulse is visible on the screen, and resized until it takes up about half of the screen. At each stage of the experiment, the entire echo pulse is recorded to the computer and kept for later processing.

At the end of the experiment, the time of flight data is extracted from each recorded waveform, and arranged to form a height versus time graph. From this, the surface tension versus concentration can be extracted.

The mixing and fluid preparation must be done manually, but the rest of the process is controlled by custom written software. For a single concentration with the current equipment and experimental setup, the entire process takes roughly 20 minutes to complete. However, this is far from an ideal setup, and experiment times could easily be driven down (see section 25).

17 Visual Observation

With the proper setup, it is possible to see the mound form and relax with the unaided eye. To accomplish this, an LED is focused at the surface of the fluid. When the mound forming pulse is sent, the falling edge of the trigger of the waveform generator starts a delay, the duration of which can be controlled by a potentiometer. At the end of the delay, the LED is flashed on, for a duration which can be controlled by a second potentiometer. If the mound creation pulse is sent at an interval of 1 Hz or less, it creates a stroboscopic effect, so that it appears visually that the mound has a constant

shape. As the delay between the mound forming pulse and the LED flash is slowly increased, the mound will visually appear to relax.

Part IV
Results and Analysis

18 Echo Return Analysis

The first piece of data that must be analyzed is the echo return signal. An echo signal is caused by the reflection of an acoustic signal at one or more interfaces. The transducer receives the echo signal, and converts it to a voltage that can be viewed on the oscilloscope. A typical echo pulse will look like Figure 10 when viewed over a large time scale. The large vertical line at time 0 is the original pulse which is sent by the transducer (See subsection 11.3). The first small bump (labeled (a) in Figure 10) represents the interface of the coupling fluid and the fluid container. The interface only partially reflects and is out of focus, and so the peak at this interface is very small. The next peak (labeled (b) in Figure 10) represents the interface between the test fluid and the air. Since air has an impedance mismatch with most liquids, much of the acoustic wave is reflected; further, since this interface is at the focal distance, the acoustic intensity is high at this point, leading to a large peak. The third bump (labeled (c) in Figure 10) represents a second reflection of the fluid surface. When the acoustic wave which is first reflected from the surface encounters the fluid container, most of the wave transmits through, leading to peak (b); however some of the wave reflects again. This reflected wave again reflects off of the surface liquid. Some of this twice reflected wave transmits through the fluid container and forms peak (c). Further reflections are small enough to be unnoticeable. Likewise, when the acoustic waves are incident upon the transducer, not all of the acoustic wave is absorbed and converted into electrical energy. Some of it is reflected and goes through the same series of reflections, giving rise to the smaller duplicate seen on the far right of Figure 10.

Since the peak at (b) represents the reflection from the surface of the liquid, it is this peak that will be analyzed to determine the time of flight of the echo pulse.

As was discussed in subsection 5.1, there is a ring-down associated with a transducer. This appears in the returned echo signal as a decaying sinusoidal curve. The characteristics of this curve are very different for either a high resolution or high sensitivity transducer. As can be seen in Figure 12, the high resolution transducer has at most a few maxima, and then falls off very quickly. For a high sensitivity transducer, on the other hand (Figure 13), the ringdown can last considerably longer. In both cases, the shape of the ringdown will change as the echo delay increases, due to self interference from the acoustic waves (compare the shapes in Figure 11).

For a high resolution transducer, it is usually sufficient to pick out the time at which the maximum occurs, and use this as total time of flight. For a high sensitivity transducer, the maximum will often shift around within the wave packet, which would cause discontinuities in the final curve if the maxima alone were selected. To find the time of flight, then, a weighted root mean square will yield a more useful result.

$$\text{Time of Flight} = \sqrt{\frac{\sum (A_t t)^2}{\sum (A_t)^2}}$$

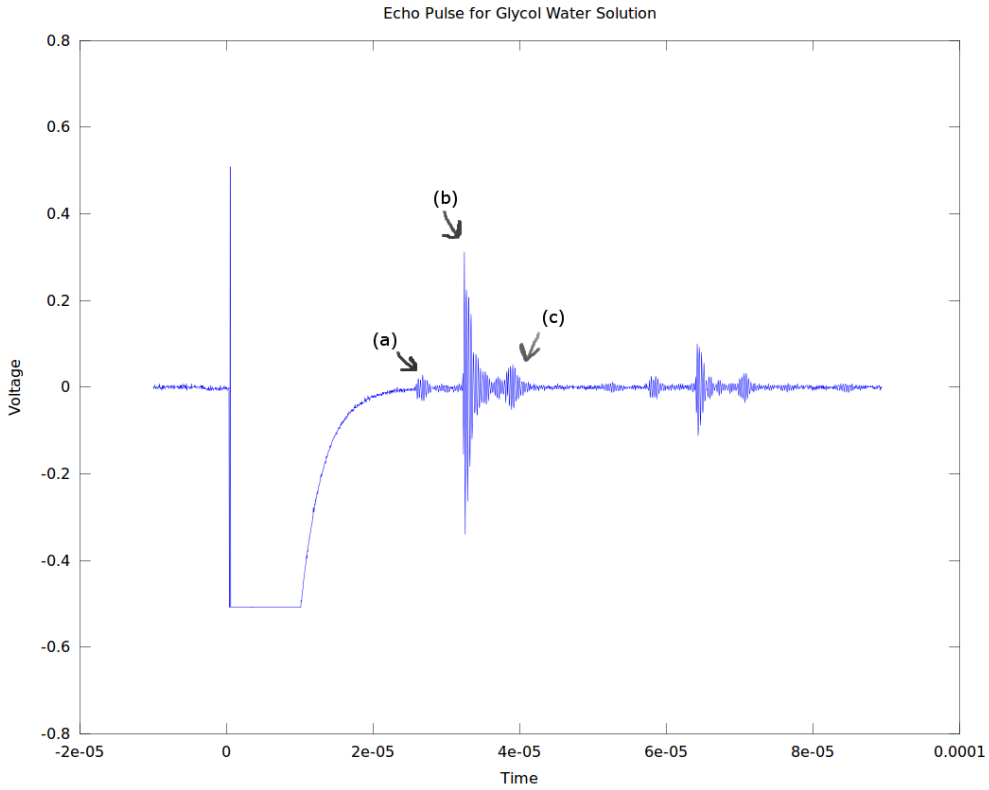

Figure 10: Echo Pulse and Reflections on Wide Timescale

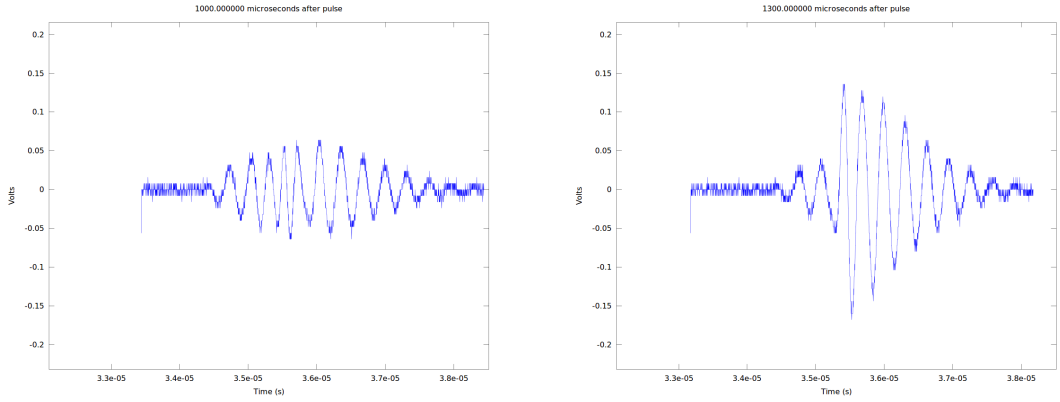

Figure 11: Ring down at different echo delays with high sensitivity transducer

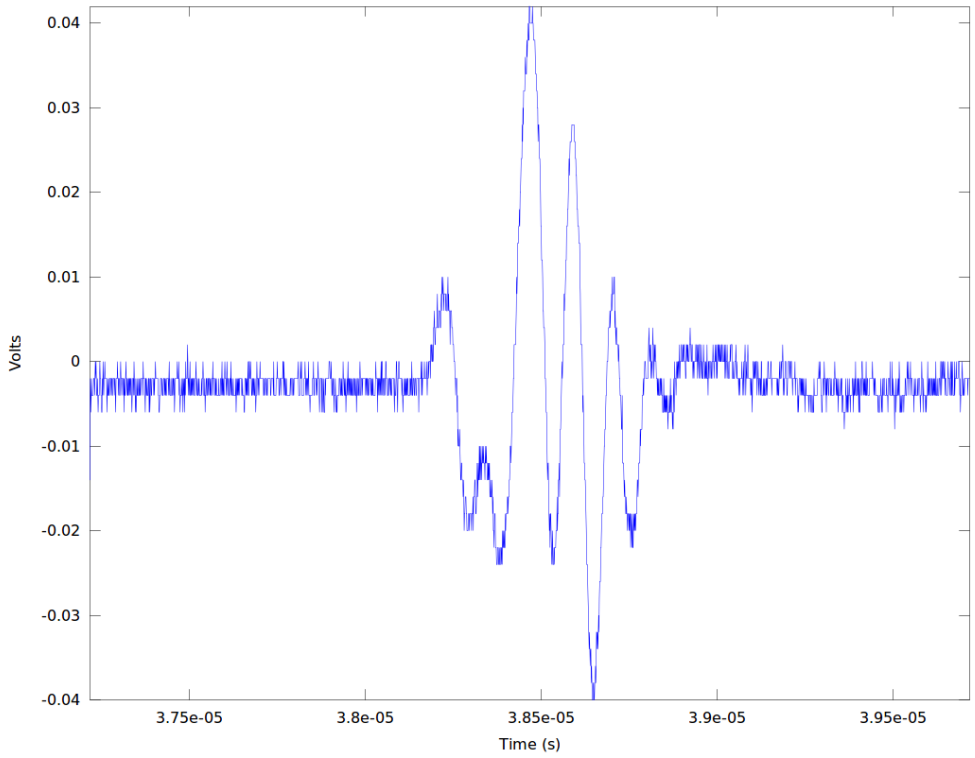

Figure 12: High Resolution Transducer Echo Signal

where A_t is the signal amplitude at time t.

19 Height vs Time Graphs

Since the echo delay is the amount of time that passes between the mound formation and the height measurements, we can arrange the height measurements by the echodelay, and get a height vs. time graph. As can be seen in Figure 14, there is a clear rise and fall of the mound. This can often be seen more clearly in a plot with a logarithmic time scale, as in Figure 14.

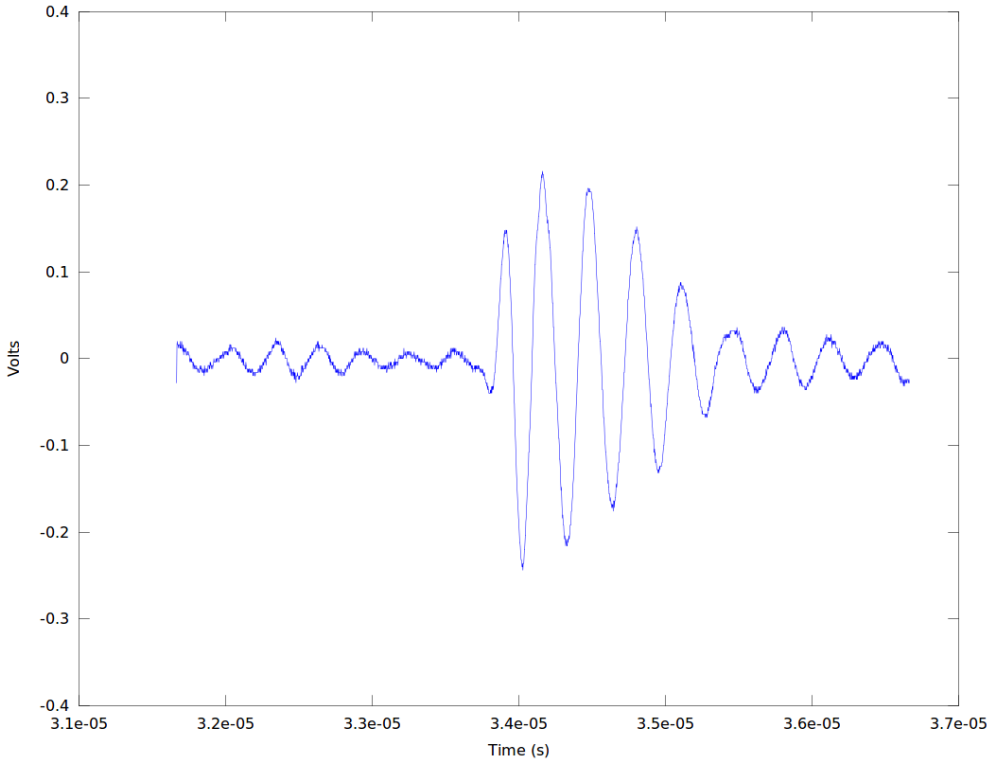

Figure 13: High Sensitivity Echo Signal

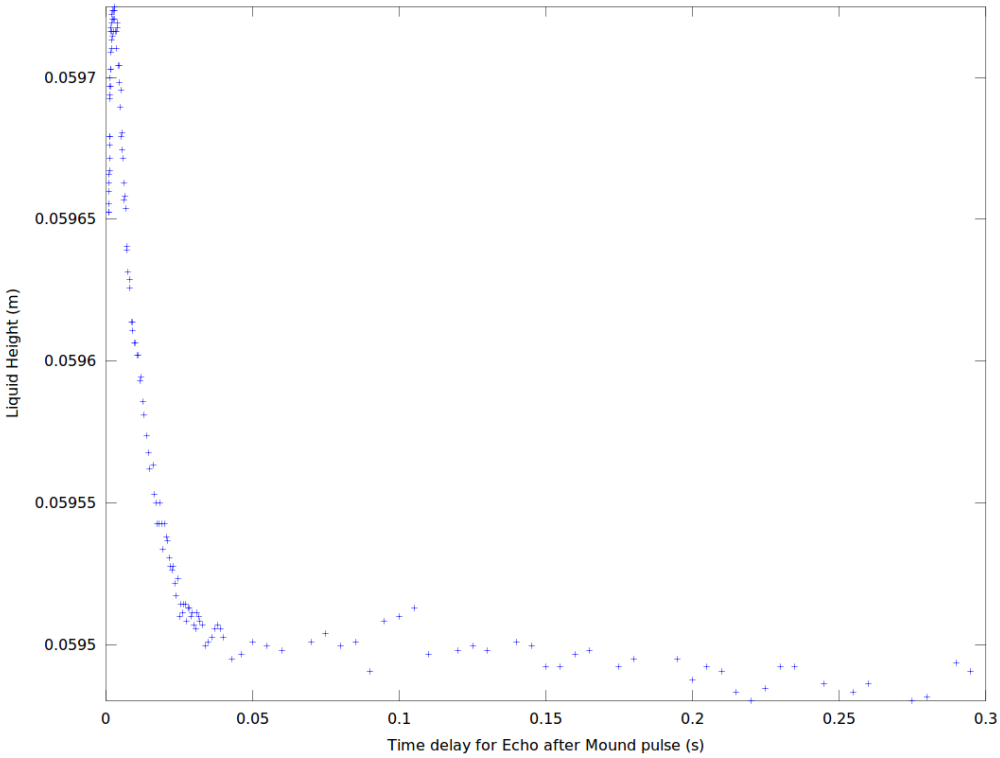

Figure 14: Relaxation curve for pure water

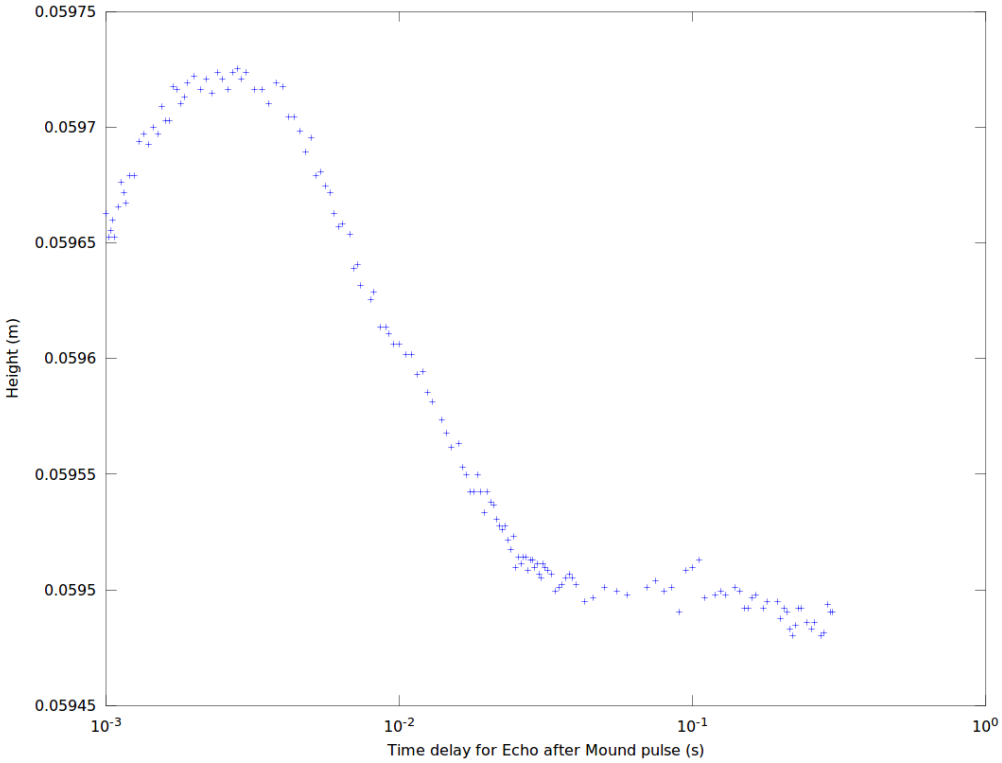

Figure 15: Relaxation curve for pure water with a logarithmic time scale

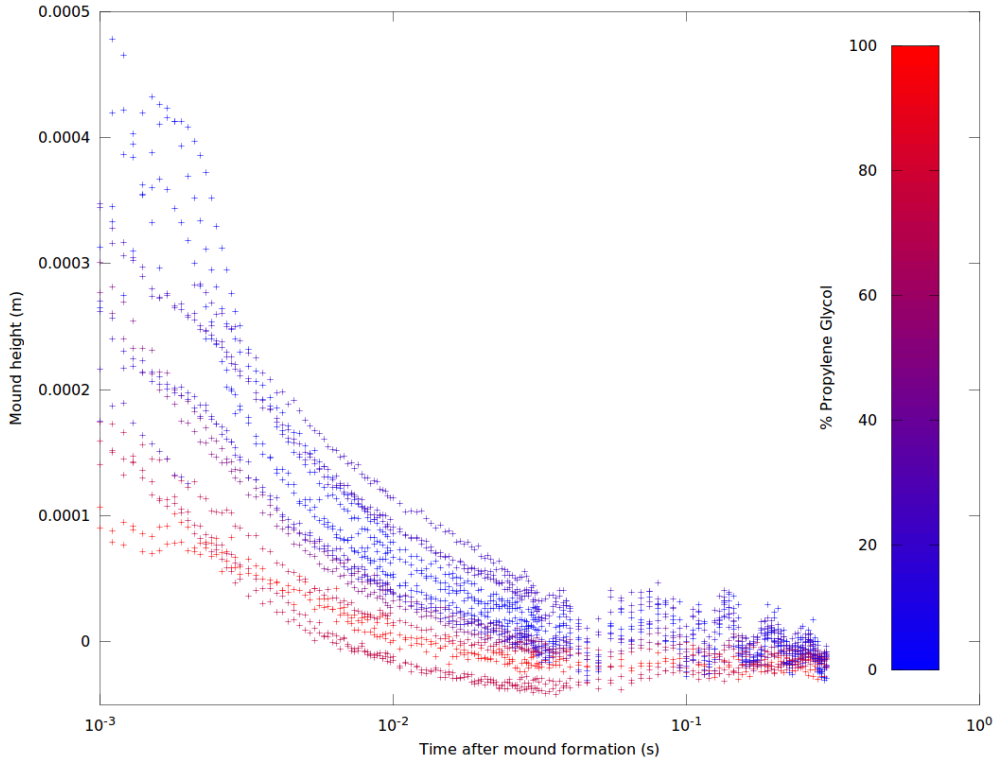

Figure 16: Rise and fall of various concentrations of aqueous propylene-glycol. Fluid directly in bubbler in contact with transducer

20 Data

20.1 Containerless

To collect this data, the solution was pipetted directly into the bubbler, placing it in contact with the transducer surface. A high sensitivity 5 MHz transducer was used with a V_{pp} of 98 volts and a pulse duration of 30 μs. The rise and fall of the mounds can be seen in Figure 16.

20.2 HDPE Milk Bottle Container - High Sensitivity

5 mL of solution was pipetted into a HDPE milk bottle cap. The bottle cap was placed on the bubbler in contact with the coupling fluid. A high sensitivity 5 MHz transducer was used with a V_{pp} of 98 Volts, and a pulse duration of 100 μs. The rise and fall of the mounds can be seen in Figure 17.

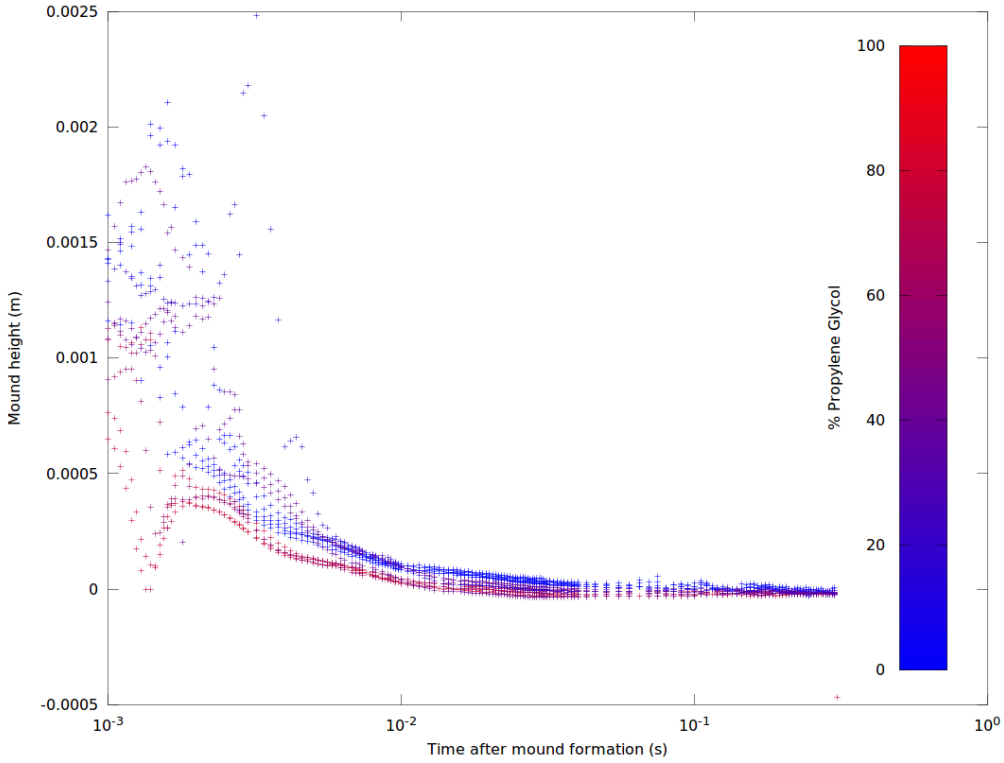

Figure 17: Rise and fall of various concentrations of aqueous propylene-glycol. High Sensitivity Transducer. Fluid in HDPE Bottle Cap

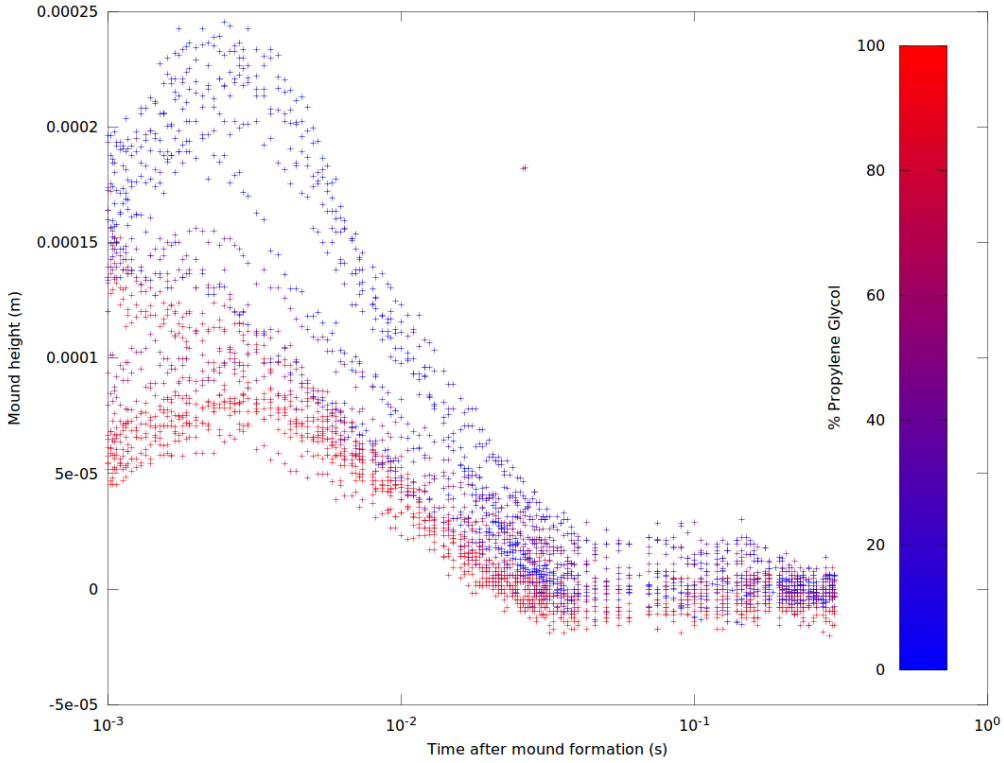

Figure 18: Rise and fall of various concentrations of aqueous propylene-glycol. High Resolution Transducer. Fluid in HDPE Bottle Cap. First Run.

20.3 HDPE Milk Bottle Container - High Resolution I

5 mL of solution was pipetted into a HDPE milk bottle cap. The bottle cap was placed on the bubbler in contact with the coupling fluid. A high sensitivity 5 MHz transducer was used with a V_{pp} of 98 Volts, and a pulse duration of 100 μs. The rise and fall of the mounds can be seen in Figure 18.

20.4 HDPE Milk Bottle Container - High Resolution II

Before this dataset was taken, the apparatus was taken apart and more carefully reassembled and realigned. The measurement and analysis software was also modified to take data more quickly. It is probably the most accurate dataset. 5 mL of solution was pipetted into a HDPE milk bottle cap. The bottle cap was placed on the bubbler in contact with the coupling fluid. A high sensitivity 5 MHz transducer was used with a V_{pp} of 98 Volts, and a pulse duration of 100 μs. The rise and fall of the mounds can

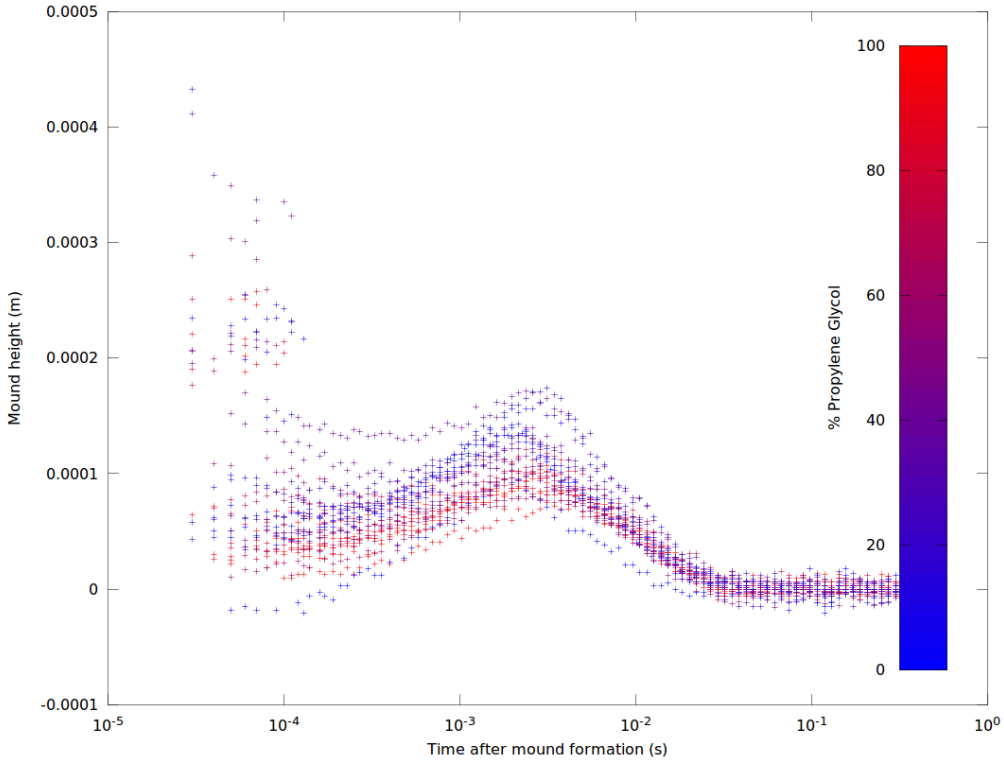

Figure 19: Rise and fall of various concentrations of aqueous propylene-glycol. High Resolution Transducer. HDPE Bottle Cap. Second Run.

be seen in Figure 19. For this run, the surface tension was calculated as a function of rise time for each concentration. The results are given in Figure 20.

21 Analysis & Discussion

All of the mound formation and relaxation curves show a clear dependence on concentration for maximum mound height. The pure water is at the top, and pure glycol is at the bottom, with the intervening concentrations between them. This is expected, since glycol has a higher viscosity than water. Thus the attenuation of the acoustic energy will be higher through glycol than through water, leaving less energy to overcome the force of surface tension. The dependence of the mound height on viscosity has not yet been entirely worked out (see section 25).

The rise time of the mound is also dependent on concentration, but this is much less clear from the graphs. Consequently, the measured surface tensions, which were

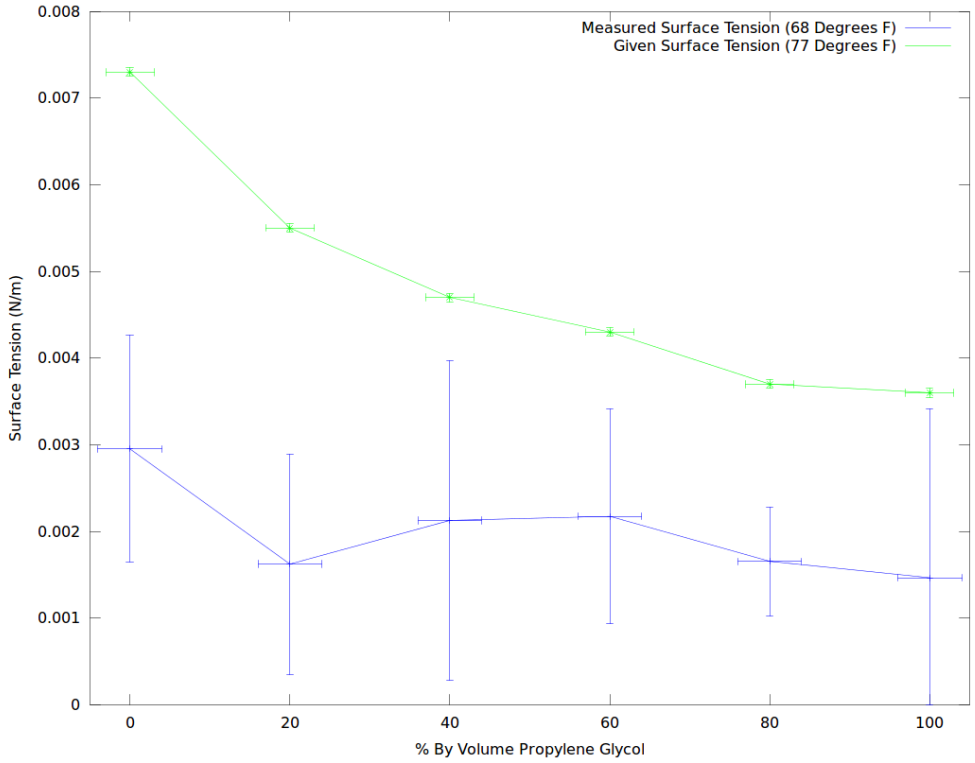

Figure 20: Surface tension vs. Concentration. High Resolution Transducer. HDPE Bottle Cap. Second Run.

derived from the rise times of the fluids, have a large uncertainty.

The measured surface tensions, however, are far from the accepted values. Even accounting for the temperature difference between the measured and given surface tensions, the measured values show large disagreement with the accepted surface tension values. This is likely due to a number of factors—perhaps most importantly an imprecisely engineered apparatus.

There was considerable difficulty in determining the focal distance of the high sensitivity transducer. It did not display a clear intensity peak at a particular focal length, so a best guess based on echo signal distance measurements and inspection of the echo amplitude was made to place the transducer roughly one inch below the liquid surface.

22 Uncertainty Analysis

A rigorous apparatus would warrant a rigorous uncertainty analysis. However, the current apparatus was more of a proof of concept test apparatus rather than a well-designed piece of scientific test equipment. A more precise design and construction would probably address many of the concerns raised in this section.

One potential source of error that was not adequately taken into account is dissolved gases. Dissolved gases can form minute bubbles in the liquid, which can interfere with the transmission of the acoustic wave, or with the motion of the liquid surface (Heuter and Bolt, 2000). The precise effects of the dissolved gases were not investigated. It may be possible to degas the liquid with an intense ultrasonic pulse, but this also was not investigated.

Another factor in the data collection is evaporation. Over time, the surface of the fluid will evaporate. Since the sizes of the mounds under consideration are very small, the change of fluid height due to evaporation will be noticeable. However, since the surface area of the entire liquid is much greater than the surface area of the mound, a linear evaporation rate can be safely assumed. It is a simple matter to continue to take height measurements after the mound has decayed, and use a linear regression to determine the rate of evaporation. The effects of evaporation can then be subtracted out of the mound decay data.

The time of flight was plotted against time immediately after fluid was poured into the bubbler using a pipette (Figure 21). No fluid container was used. It appears that the fluid takes some time to settle in to the bubbler before a linear evaporation takes over.

Probably the most significant sources of error, however, were the levelness of the transducer and interfaces, and the distance of the surface from the focus of the transducer. If the transducer is not completely vertical, there are many things that can happen to the acoustic energy. First, if the transducer axis is not aligned with gravity, a mound may form, but since gravity will not be pulling it uniformly downward, it may be come lopsided, leading to unpredicted mound formation and decay. Second, the acoustic echoes will be reflected at an angle, leading to longer times of flight than for a straight perpendicular flight path. If the transducer is not aligned with the bubbler, some of the acoustic wave may reflect off the walls of the bubbler, leading to a loss

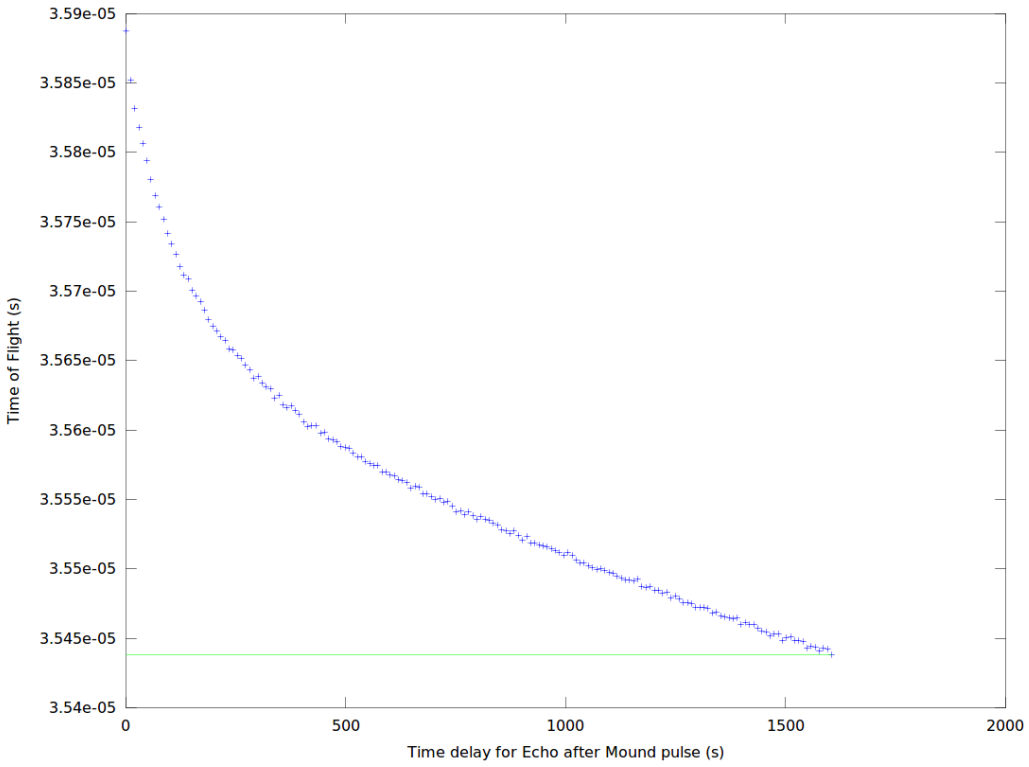

Figure 21: Time of flight immediately after fluid poured into bubbler

of focus, or even multiple focal spots. If the transducer axis is not perpendicular to the fluid container, not all of the acoustic energy will be transmitted in the normal direction, some will be transmitted in the transverse direction, inciting shear waves in the fluid container, which in turn could set up low frequency standing waves in the liquid surface.

Another factor that was not adequately considered was the inclusion of the pulse duration in the rise time. Presently, the rise time is given with respect to the end of the mound forming pulse. It may be that the rise time should be with respect to the beginning of the mound forming pulse, which would cause a difference of $\approx 500\mu$s. Further, the time of each height measurement is currently counted as the time at which the echo pulse is sent. A more accurate measurement may be to count the time of the height measurement as the time at which the echo pulse is sent plus the time it takes to reach the top of the mound.

23 Anomalies

23.1 Inverted Relaxation Curve

When the surface is exactly in focus, the height curve will start out below the rest position and then steeply rise, rather than fall. This can be seen in Figure 22. Rather than the time of flight of the echo pulses rapidly decreasing, as is expected of a relaxing mound, the time of flight actually increases.

The first attempt at a reasonable explanation of this phenomena might be that the mound is so small that the echo does not reach the top of the mound, but rather reflects off of the fluid displaced to form the mound. As was said in subsection 9.1, the minimum mound diameter will occur when the transducer is exactly in focus. In this case, the diameter of the mound will be about the size of one wavelength. As this fluid rises, it will create a pressure differential, causing the surrounding fluid to lower and fill the space. This will cause the surrounding fluid to be lower than the mound created. If the surrounding fluid interferes with the echo pulse, it will capture the trajectory of the surrounding fluid rising, rather than the mound falling.

This hypothesis was checked by focusing the transducer until an inverse relaxation curve was obtained, and then changing the transducer height so that it was slightly out of focus. After the focus was changed, the inverse relaxation curve went away.

However, additional data was later taken with the transducer up to an inch out of focus, and inverted curves were still obtained. However, it was noticed that the surface of the entire fluid (which has the surface area of the top of the petri dish) visibly vibrated when this inverted curve was obtained. Since for these vibrations to be visible, they would need to be on the order of millimeters, they would trump any hundred micrometer order mound. When the duration of the pulse was reduced, leading to less total power transmitted, both the visible vibration and the inverted relaxation curve diminished or disappeared.

A second attempt at interpreting this phenomena would be that shear waves or lower modes of vibration are being set up. This may be due either to the transducer not being

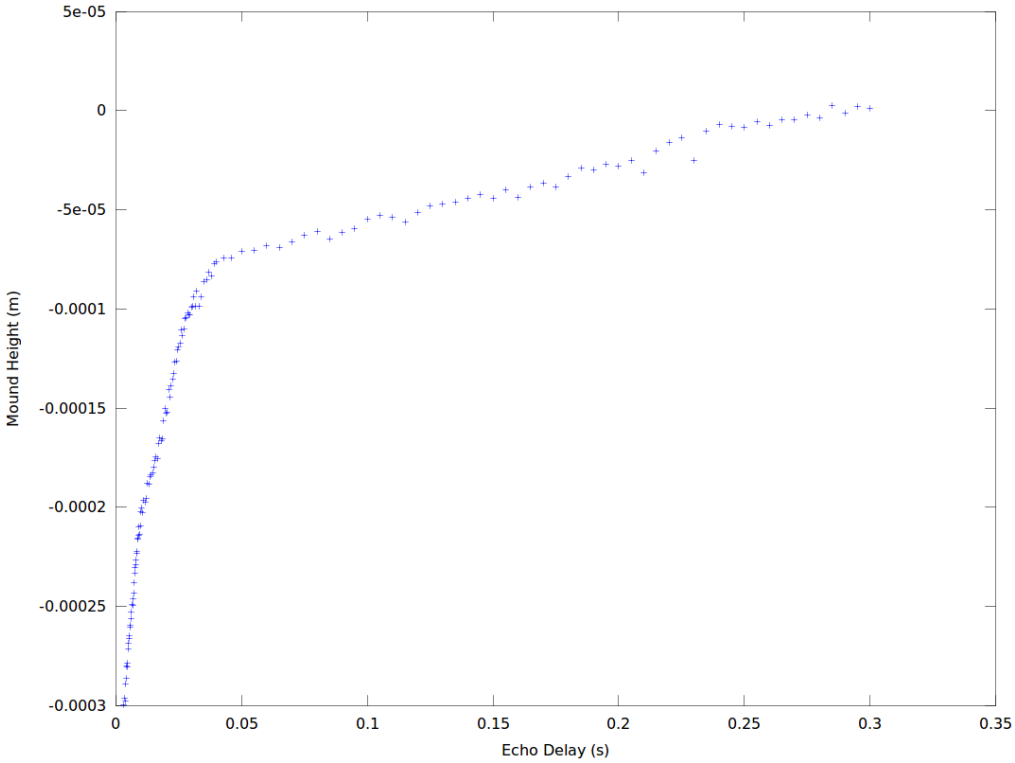

Figure 22: Inverted Relaxation Curve

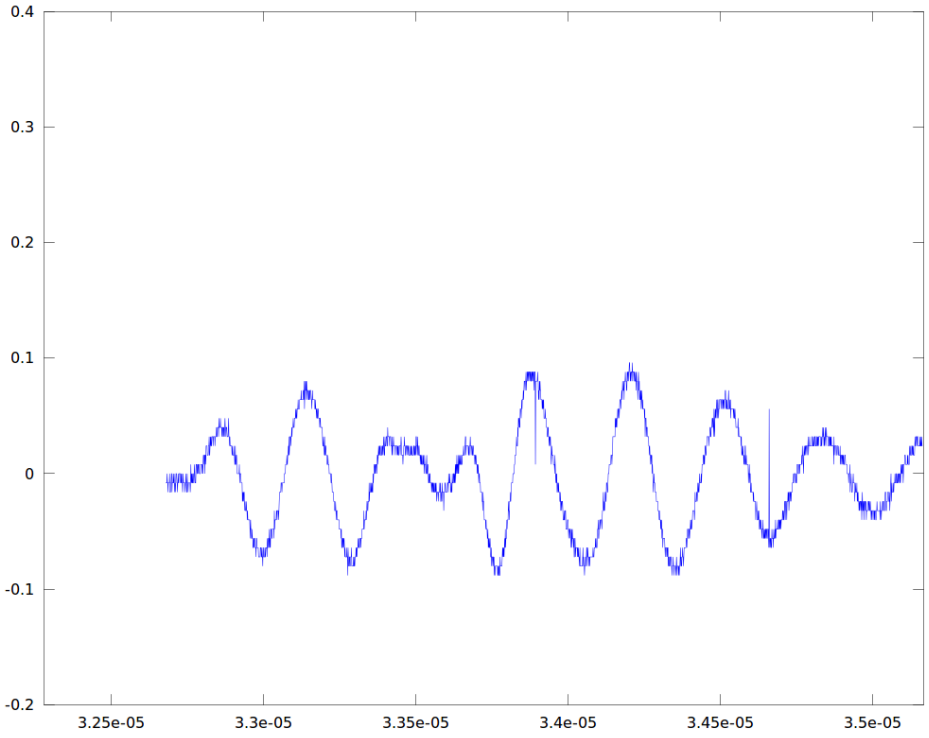

Figure 23: Echo pulse surface reflection breaking into two parts

perpendicular to the fluid surface, or due to too much power being transferred, setting up standing waves.

At this point, however, this explanation is still merely conjecture. More data is needed to determine whether this conjecture is correct.

23.2 Mound Shape Shifting

The shape might possibly be due to the wave interfering with itself from within the mound. Since the top of the mound will be smaller than the bottom of the mound due to the roughly Gaussian shape of the mound (Elrod et al., 1989), the top of the mound will be smaller than the wavelength of the acoustic wave. This will cause all sorts of interference. It may be possible to analyze this interference, and figure out something of the shape of the mound, but more research is needed in this area.

One especially useful place where this might occur is during droplet ejection. In Figure 23, it appears that the mound is splitting into two separate mounds. This came from a mound that have had enough energy to begin forming a droplet. If the echo

delay were to be increased, the two echo bumps would either get farther away until they separated, which would indicate droplet formation, or they would get closer together until they were indistinguishable, which would indicate that no droplet was formed. By analyzing this further, it may be possible to devise a system to detect if droplets have been formed.

Part V
Conclusion

24 Conclusion

While this method is not yet as robust or accurate as other methods, it shows a lot of promise. With a better setup, better results could be obtained. If the uncertainty and the error in these results can be reduced enough, then this technique could prove a very powerful and agile technique for fluid property measurements.

25 Future Research

25.1 Apparatus

The most immediate area for improvement is the design and construction of the apparatus. While the oscilloscope has sufficiently high resolution to record a single echo pulse, its data transfer speed limits the experiment to one echo pulse (and consequently height measurement) per mound formation. If an upgraded data acquisition unit were used, which could either transmit the data at real time speeds, or capture the entire 3 millisecond rise and relaxation of a mound, multiple echoes could be sent per mound, greatly increasing the speed of the experiment. In the ideal case, one echo could be sent out immediately as the previous echo is returned. If an adjustable initial offset is used, a very accurate measurement of the formation and relaxation of the curve could be taken by adjusting the initial offset very slightly each time, so that instead of forming 150 mounds, only 5 or 10 mounds would need to be formed. The experiment would then last on the order of seconds rather than the order of tens of minutes.

The other obvious construction improvements involve leveling, and ensuring perpendicularity. Currently, the transducer holder is a clamp attached to a cylindrical post, which has a tendency to twist and slide. A better design would include a mechanism to keep both the transducer and bubbler aligned with gravity.

25.2 Viscosity

Some theoretical work remains to derive the dependence of maximum mound height on viscosity. Since the maximum mound height is proportional to the energy incident on the surface, measuring the mound height and the energy emitted by the transducer should reveal how much energy has been lost in transit. One would then have to account for energy lost at the interfaces between the coupling fluid and the fluid container as well.

A start to a derivation of relative viscosity of some glycol solution η_g relative to pure water η_w given maximum mound heights for both h_g and h_w, is listed below. The advantage of using a relative measurement is that the properties of the intervening

materials, such as the fluid container, need not be known as long as they are the same for both the measurements for water and the test fluid.

$$\begin{aligned}
\frac{h_g}{h_w} &= \frac{0.21\dfrac{E_g^2 f^4}{c_g^6 \sigma_g \rho_g}}{0.21\dfrac{E_w^2 f^4}{c_g^6 \sigma_w \rho_w}} \\
&= \frac{\dfrac{I_0 e^{-2\alpha_g d} AT}{c_g^6 \sigma_g \rho_g}}{\dfrac{I_0 e^{-2\alpha_w d} AT}{c_g^6 \sigma_w \rho_w}} \\
\frac{h_g}{h_w}\frac{c_w^6 \sigma_w \rho_w}{c_g^6 \sigma_g \rho_g} &= e^{2\alpha_w d + 2\alpha d} \\
2\alpha_w d - 2\alpha_g d &= \ln\left(\frac{h_g}{h_w}\frac{c_w^6 \sigma_w \rho_w}{c_g^6 \sigma_g \rho_g}\right) \\
\alpha_g &= \alpha_w - \frac{1}{2d}\ln\left(\frac{h_g}{h_w}\frac{c_w^6 \sigma_w \rho_w}{c_g^6 \sigma_g \rho_g}\right) \\
\frac{2}{3}\frac{\eta_g}{\rho_g}\frac{f}{c_g^2} &= \frac{2}{3}\frac{\eta_w}{\rho_w}\frac{f}{c_w^2} - \frac{1}{2d}\ln\left(\frac{h_g}{h_w}\frac{c_w^6 \sigma_w \rho_w}{c_g^6 \sigma_g \rho_g}\right) \\
\eta_g &= \frac{3}{2}\frac{\rho_g c_g^2}{f}\left[\frac{2}{3}\frac{\eta_w}{\rho_w}\frac{f}{c_w^2} - \frac{1}{2d}\ln\left(\frac{h_g}{h_w}\frac{c_w^6 \sigma_w \rho_w}{c_g^6 \sigma_g \rho_g}\right)\right]
\end{aligned}$$

E_x	Energy at surface of x
f	Wave frequency
c_x	Speed of sound of x
σ_x	Surface tension of x
ρ_x	Density of x
α_x	Viscous decay constant of x
I_0	Initial intensity at bottom of liquid
d	Distance traveled in liquid
η_x	Shear viscosity of x

where x is either g for the glycol solution, or w for water.

This equation, besides being very messy, requires knowledge of the density, surface tension, and speed of sound of the material to be measured. The surface tension can be measured using the mound rise time, and density and speed of sound measurements are standard procedures. A significant advancement of this project would be to combine surface tension, viscosity, speed of sound, and density measurements into a single non-contact apparatus.

26 Acknowledgments

First and foremost, this research owes its inception and much of its completion to the ingenuity of my thesis advisor, Dr. David Lee. Dr. Lee's tireless efforts to direct me to answers to difficult questions and solutions to difficult problems. His wide expertise in the area and beneficial industrial contacts provided immeasurable assistance in the project.

Thanks is also due to the rest of the Gordon College Physics department, both faculty and students. Special thanks is due to Professor Stan Reczek for advice and assistance in some mechanical construction for the project. A special thank you is due to my research group consisting of Jesse Thompson, Darrell Montonerra, Danielle Duggins, Nathan Bedell and Stephen Collins. Many long, arduous hours were spent working side by side in the labs. A warm thanks as well is extended to the rest of the physics students, with whom were spent many late nights working on this research.

The Gordon College Chemistry Department, both faculty and students, provided expertise and equipment, both of which proved quite important in the completion of this project.

Andy Bartfay graciously designed and built the pulser amplifier circuit, which provided a tremendous boost to completing the project on time.

Finally, much thanks and gratitude are due to the rest of my friends and family who have supported my work, and tolerated my nearly complete disappearance from life during the completion this project.

Thanks everyone.

References

Cinbis, C. and Khuri-Yakub, B. T. (1992). A noncontacting technique for measuring surface tension of liquids. *Rev. Sci. Instrum*, 63(2).

Cinbis, C., Mansour, N. N., and B, T. K.-Y. (1993). Effect of surface tension on the acoustic radiation pressure-induced motion of the water-air interface. *Journal of the Acoustical Society of America*, 94(4).

Dryer, R., Browning, B., and Vlahos, H. (2011). Access laboratory workstation: A novel approach to quickly and easily add automation to echo liquid handlers. Poster.

du Noüy, P. L. (1925). An interfacial tensiometer for universal use. *The Journal of General Physiology*, 7(5):625–631.

Elrod, S. A., Khuri-Yakub, B. H. B. T., Rawson, E. G., Richley, E., Quate, C. F., Mansour, N. N., and Lundgren, T. S. (1989). Nozzleiess droplet formation with focused acoustic beams. *Journal of Applied Physics*, 65(9).

Enflo, B. O. and Hedberg, C. M. (2002). *Theory of nonlinear acoustics in fluids*. Kluwer Academic Publishers, Boston.

Heuter, T. F. and Bolt, R. H. (2000). *Sonics*. Acoustical Society of America.

Hon, S. (2009). Study of self-focused piezoelectric transducer for liquid ejection. Master's thesis, The Hong Kong Polytechnic University, http://hdl.handle.net/10397/2654.

Huh, C. and Reed, R. L. (1983). A method for estimating interfacial tensions and contact angles from sessile and pendant drop shapes. *Journal of Colloid and Interface Science*, (2).

Inouchi, M. and Shibata, M. (2008). Fish finder that transmits ultrasonic waves, receives echo signals, and performs interference removal. US Patent No. 7388809.

Koseli, V., Zeybek, S., and Uludag, Y. (2006). Online viscosity measurement of complex solutions using ultrasound doppler velocimetry. *Turkish Journal of Chemistry*, pages 297–305.

Dow Chemical Company (2003). *Guide to Glycols*. http://www.dow.com/PublishedLiterature/dh_0047/0901b803800479d9.pdf?filepath=propyleneglycol/pdfs/noreg/117-01682.pdf&fromPage=GetDoc.

FLEXIM (2006). *Sound Speed of Various Media*.

NASA (1998). *Manipulation of Liquids by Use of Sound*. Clevland, Ohio. NASA Tech Briefs.

NDT International, Inc. (2010). *Basic Ultrasonic Principles*. http://www.ndtint.com/Basic%20UT%20Principles.PDF.

Nilsson, J. W. and Riedel, S. A. (2011). *Electric Circuits*. Prentice Hall.

Nowicki, A., Secomski, W., and Wojcik, J. (1997). Acoustic streaming: Comparison of low-amplitude linear model with streaming velocities measured by 32-mhz doppler. *Ultrasound in Medicine and Biology*, 23(5).

Parkin, S. J., Knöner, G., Nieminen, T. A., Heckenberg, N. R., and Rubinsztein-Dunlop, H. (2007). Picoliter viscometry using optically rotated particles. *ArXiv e-prints*, 76(4):041507.

Rame, E. (1996). The interpretation of dynamic contact angles measured by the wilhelmy plate method. *Journal of Colloidal and Interface Science*, 185:245–251.

Vikram Singh, A., Sharma, L., and Gupta-Bhaya, P. (2012). Studies On Falling Ball Viscometry. *ArXiv e-prints*.

Wilke, J., Kryk, H., Hartmann, J., and Wagner, D. (2000). *Theory and Praxis of Capillary Viscometry*. SCHOTT.

Appendices

Appendix A: Pulser Circuit

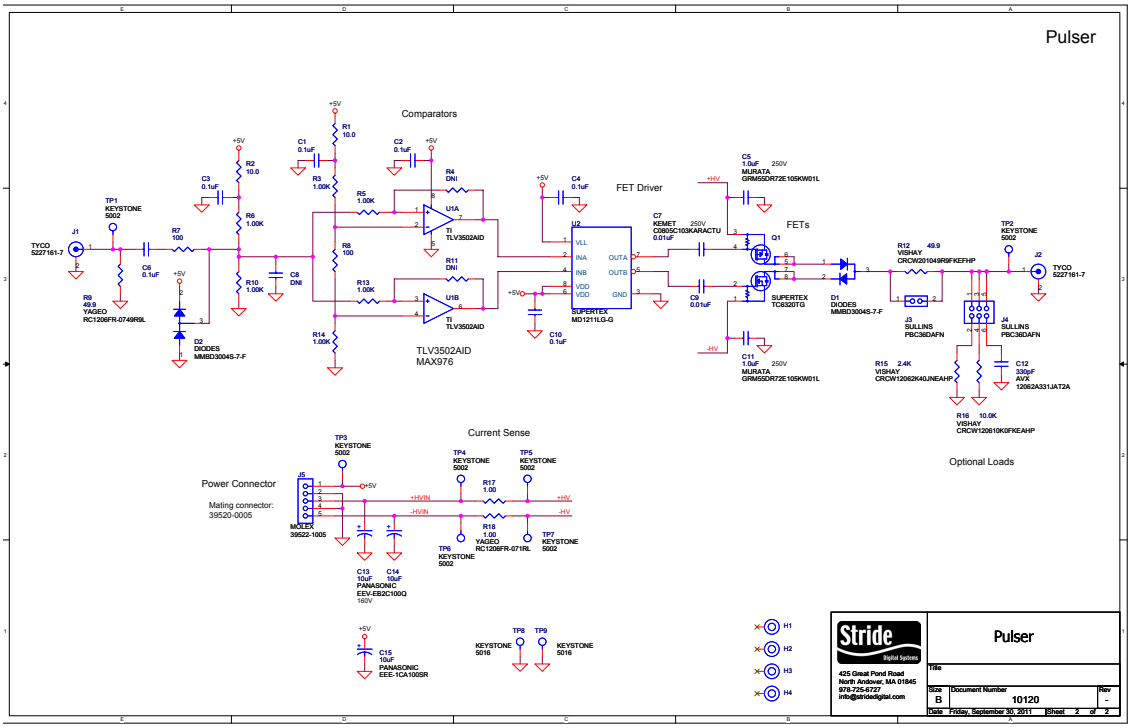

Figure 24: Pulser Circuit Schematic

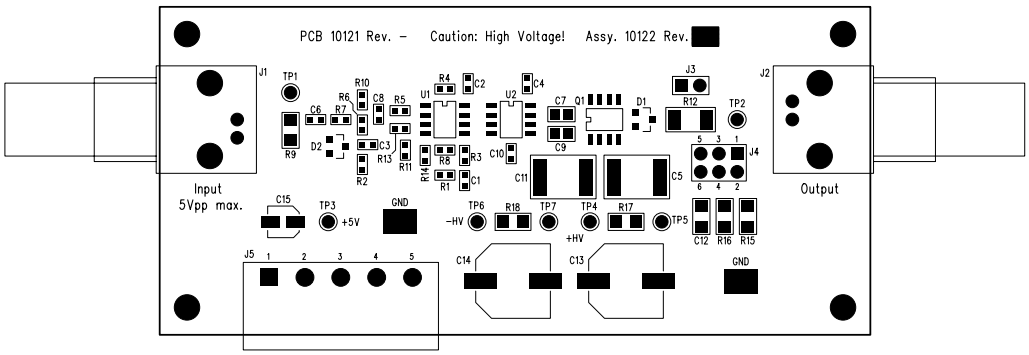

TOP SIDE SILK SCREEN

LAYER 1/TOP

Figure 25: Pulser Circuit Board Diagram

Appendix B: Variable Delay Strobe Circuit

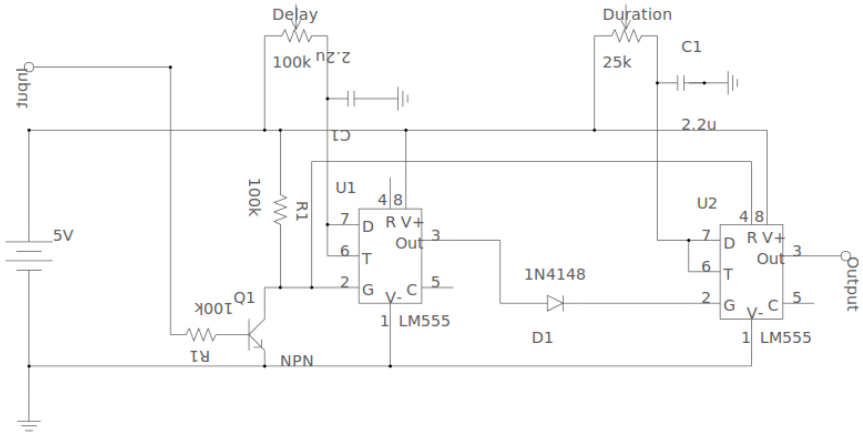

Figure 26: Variable Delay Strobe Circuit Schematic

Appendix C: Detailed Setup Diagram

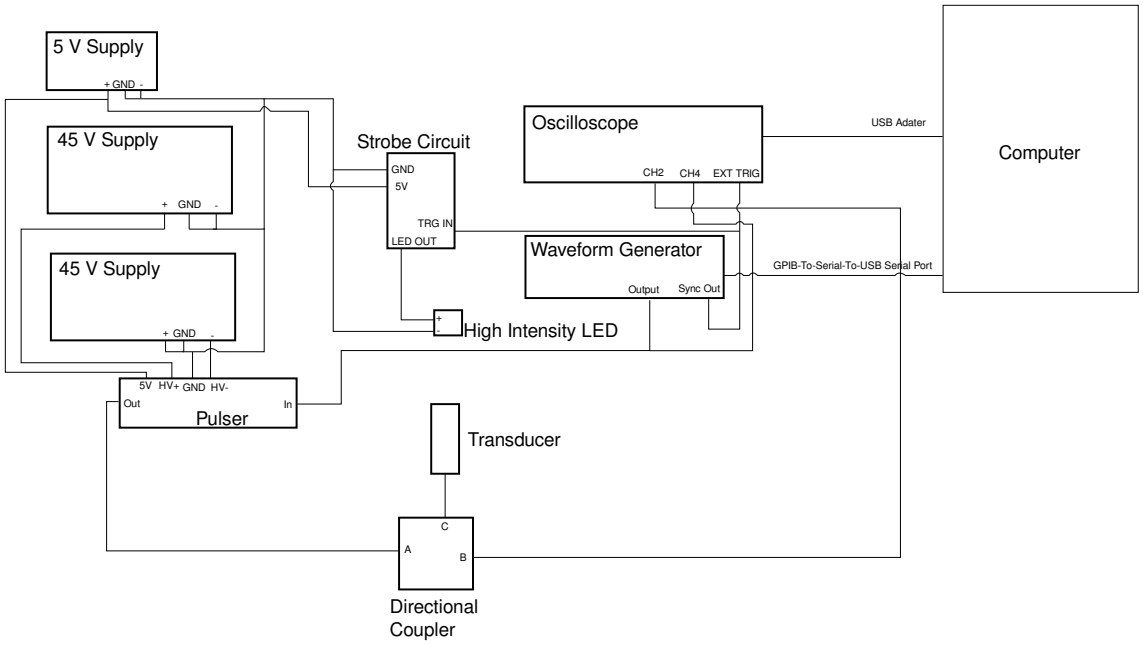

Figure 27: Detailed Wire Connection Diagram

Appendix D: Control and Analysis Code

The control and analysis source code can be found in the ADE Project folder on the physics file server, or in the physics subversion repository.